GDCh

Reviews

Angewandte
Chemie
International Edition
www.angewandte.org

Photochemistry

Charge-Transfer and Spin-Flip States: Thriving as Complements

*Winald R. Kitzmann and Katja Heinze**
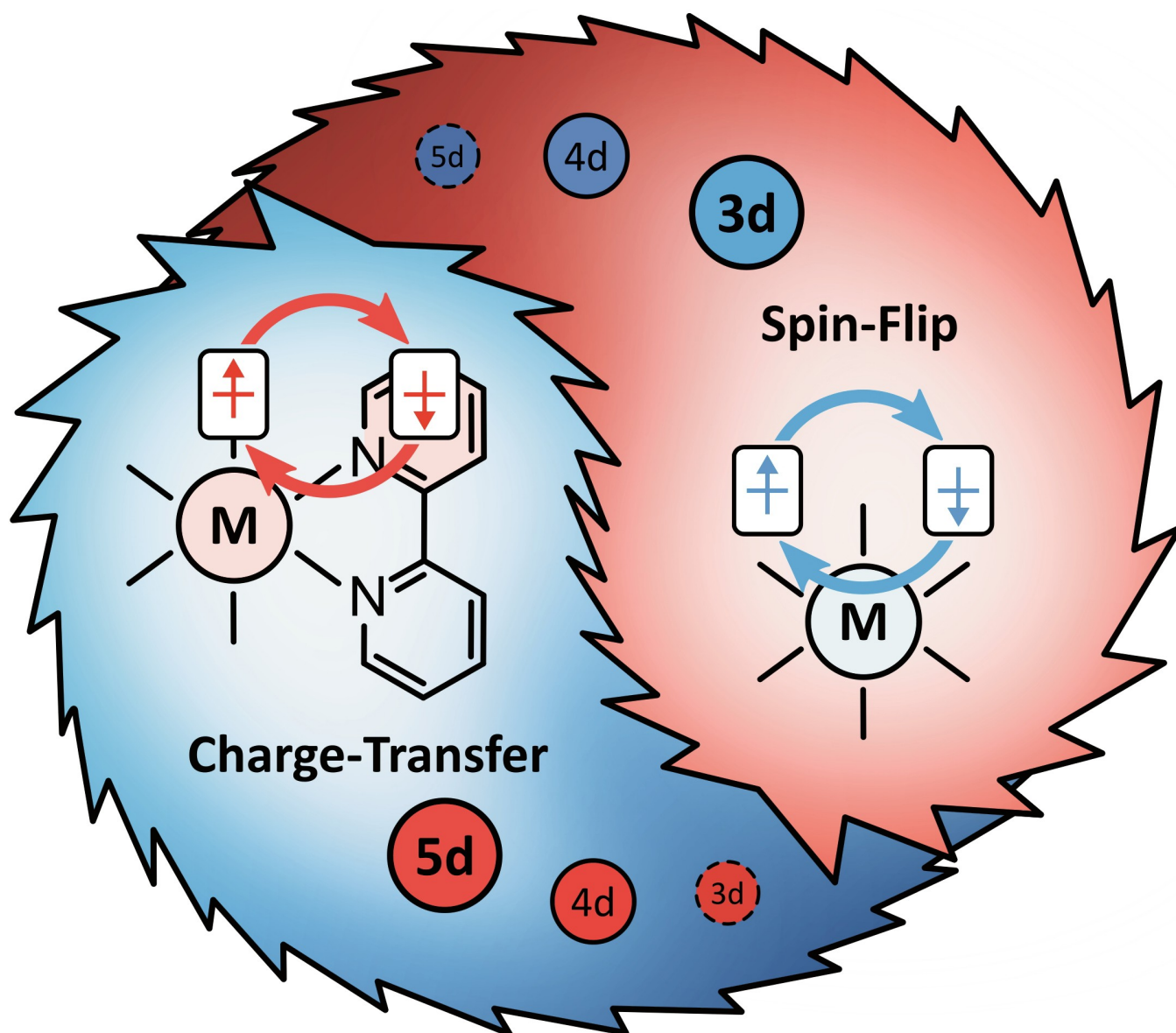
Abstract: Transition metal complexes with photoactive charge-transfer excited states are pervasive throughout the literature. In particular, $[Ru(bpy)_3]^{2+}$ (bpy = 2,2′-bipyridine), with its metal-to-ligand charge-transfer emission, has been established as a key complex. Meanwhile, interest in so-called spin-flip metal-centered states has risen dramatically after the molecular ruby $[Cr(ddpd)_2]^{3+}$ (ddpd = N,N′-dimethyl-N,N′-dipyridin-2-yl-pyridine-2,6-diamine) led to design principles to access strong, long-lived emission from photostable chromium(III) complexes. This Review contrasts the properties of emissive charge-transfer and spin-flip states by using $[Ru(bpy)_3]^{2+}$ and $[Cr(ddpd)_2]^{3+}$ as prototypical examples. We discuss the relevant excited states, the tunability of their energy and lifetimes, and their response to external stimuli. Finally, we identify strengths and weaknesses of charge-transfer and spin-flip states in applications such as photocatalysis and circularly polarized luminescence.

1. Introduction

Photoactive and (often) emissive transition metal complexes are of high interest for fundamental research[1–5] as well as applications such as photocatalysis,[6–10] sensing,[11–13] and solar-energy conversion.[14,15] In many cases it is insufficient to select a complex for a certain use solely based on simple parameters such as the energy, lifetime, and redox potential of the excited state or its photoluminescence quantum yield.
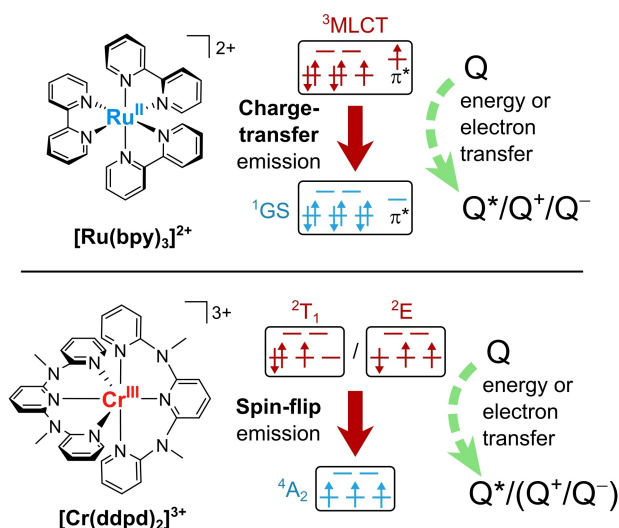

Figure 1. Chemical structures and electronic configurations of the ground and excited states involved in luminescence and excited-state reactions for the prototypical charge-transfer (CT) emitter $[Ru(bpy)_3]^{2+}$ (top) and spin-flip (SF) emitter $[Cr(ddpd)_2]^{3+}$ (bottom). Schematic representations of the quenching reactions of the excited states with a generic quencher molecule Q are shown. ^{3}MLCT and SF states can be quenched oxidatively, reductively, or through energy transfer, thereby resulting in a reduced (Q^-), oxidized (Q^+), and electronically excited quencher (Q^*), respectively.

[*] W. R. Kitzmann, Prof. Dr. K. Heinze
   Department of Chemistry, Johannes Gutenberg University of Mainz
   Duesbergweg 10–14, 55128 Mainz (Germany)
   E-mail: katja.heinze@uni-mainz.de

Instead, a deep understanding of the underlying photophysical properties of the involved excited states and of the excited-state dynamics is essential, as specific types and properties of excited states are required in different contexts.[3,16–18]

Traditionally, investigating and exploiting charge-transfer (CT) excited states was the main focus thanks to their tunability and versatility in different applications.[19–23] The most prominent examples are the 4d and 5d metal complexes $[Ru(bpy)_3]^{2+}$, first reported in 1936 by Burstall (bpy = 2,2′-bipyridine, Figure 1),[24] and Ir(ppy)$_3$, first reported in 1985 by Watts (ppy$^-$ = anion of 2-phenylpyridine, Figure 2),[25] which show intense long-lived phosphorescence arising from triplet metal-to-ligand CT (^{3}MLCT) states with quantum yields Φ and excited-state lifetimes τ of $\Phi = 9.5\%$ and several hundred nanoseconds and $\Phi = 40\%$ and $\tau = 1.9\,\mu s$, respectively, under O$_2$-free conditions.[26–29] Thousands of articles and dozens of reviews cover these complexes and their derivatives.[16,28–42]

The MLCT states can be described in a first approximation by an oxidized metal center and a ligand radical anion, namely through depopulation of a metal d orbital (t_{2g}) and population of a ligand π^* orbital (Figure 1). On the other hand, occupation of M–L antibonding d orbitals (e_g^*) gives rise to metal-centered (MC) excited states, for example in the Ru^{II} and Ir^{III} low-spin d^6 systems. These MC excited states are strongly distorted and thus facilitate nonradiative deactivation of the ^{3}MLCT states when populated.[32] Hence, MC states are commonly considered "parasitic" and detrimental to the emission and bimolecular reactivity of the excited states.[4,42–44] In complexes of the noble metal ions ruthenium(II) and iridium(III), for example $[Ru(bpy)_3]^{2+}$ and Ir(ppy)$_3$, these MC states are typically higher in energy than the ^{3}MLCT states because of the primogenic effect.[3,45,46] Homologous complexes of the base metals (3d metals) such as iron(II) are typically nonluminescent and unsuited for bimolecular reactions in their excited states because of efficient decay via low-energy MC states.[32,47,48]

The detrimental MC states in question are so-called *inter*-configurational states, which means that they have a different electronic configuration than the ground state (GS), for example, through the occupation of antibonding e_g^* orbitals in a d-d transition.

In contrast, certain electronic configurations such as d^3 in an octahedral ligand field give rise to *intra*-configurational MC states. As the name implies, the electron configuration does not change with respect to the GS. Instead, these

excited states just feature one flipped electron spin in a first approximation without changing the bonding situation and without significantly changing the geometry (Figure 1). These weakly distorted intra-configurational MC states can show phosphorescence with very long lifetimes (µs to ms), with the so-called spin-flip (SF) emission contrasting the essentially nonluminescent inter-configurational distorted MC states.[49] It is important to note, that while phosphorescence of any kind (e.g. from ^{3}MLCT states) always implies a change in multiplicity and thus the flipping of an electron spin, SF phosphorescence *only* consists of a spin-flip with no change in the electron configuration.

The most prominent example of a SF emitter is the gemstone ruby Al_2O_3:Cr^{3+}, which shows intense red phosphorescence at 694 nm with a quantum yield of $90 \pm 5\%$ and an excited-state lifetime of 4.27 ms.[50–52] Molecular Cr^{III} complexes such as $[Cr(bpy)_3]^{3+}$ and $[Cr(tpy)_2]^{3+}$ (tpy = 2,2′:6′,2′′-terpyridine, Figure 2) have been known for decades, but their performance did not live up to their solid-state counterparts. The highest quantum yield in water of 0.15% was reported for $[Cr(phen)_3]^{3+}$ (phen = 1,10-phenanthroline, Figure 2).[49,53–58]

In 2015, the polypyridine chromium(III) complex [Cr-(ddpd)$_2$]$^{3+}$ (ddpd = N,N'-dimethyl-N,N'-dipyridin-2-yl-pyridine-2,6-diamine, Figure 1) was reported to show a strong, sharp, dual phosphorescence at 738 and 775 nm, with an exceptionally high quantum yield of 13.7% and an excited-state lifetime of 1.12 ms in acetonitrile solution.[59–61] The secret to its success is the ligand ddpd, which forms six-membered chelate rings with the chromium(III) ion in an almost ideal octahedral coordination geometry. The resulting large ligand-field splitting shifts the detrimental inter-configurational MC states to a high enough energy to avoid nonradiative deactivation of the emissive SF states through back intersystem crossing (ISC).[59,62] This complex turned out to be the prototype for a new class of highly emissive and photoactive Cr^{III} complexes, the "molecular rubies", all of which rely on the above-mentioned design strategy.[63–69]

SF emission is, however, not limited to Cr^{III} complexes nor d³ electronic configurations. In fact, d², d⁴, and d⁸ electron configurations also give rise to SF states.[49] Examples using V^{III},[70–73] Mo^{III},[74,75] W^{III},[74] Cr^{IV},[76,77] Mn^{IV},[78] and Re^{IV}[75] have been reported, but with the exception of

their use as optically addressable qubits,[73,76,79] their applications are not as advanced as for molecular rubies. Nonetheless, all these complexes share the typical characteristics of SF emission.[49]

This Review describes the fundamental differences between CT and SF excited states and their applications. After introducing the optical properties of and photophysical processes in $[Ru(bpy)_3]^{2+}$ and $[Cr(ddpd)_2]^{3+}$ as prototypical and well-understood CT and SF emitters, respectively, we compare their traits and highlight advantages for different applications.

2. Electronic Nature of Charge Transfer and Spin-Flip States

In a simple picture, the electronically excited states of most mononuclear transition metal complexes can be categorized in three groups: metal-centered (MC), ligand-centered (LC), and charge-transfer (CT) states. MC states only involve the d orbitals of the metal center, LC states include transitions between ligand-based orbitals (e.g. π-π* and n-π* transitions), and CT transitions can be understood as intramolecular redox processes. The names for the CT states are derived from the nature of the donating and accepting orbitals. In a metal-to-ligand CT (MLCT) transition, an electron is transferred from metal-based d orbitals to a ligand-based π* orbital. This formally results in an oxidized metal center and a ligand radical anion. Other types of CT states include ligand-to-metal CT (LMCT), ligand-to-ligand CT (LL′CT), and intraligand CT (ILCT).[48]

MC states are further differentiated in inter-configurational and intra-configurational states that show a different or the same electronic configuration as the GS, respectively. In the following, we will refer to intra-configurational states as SF states, as they only differ from the GS by a flipped electron spin.[49]
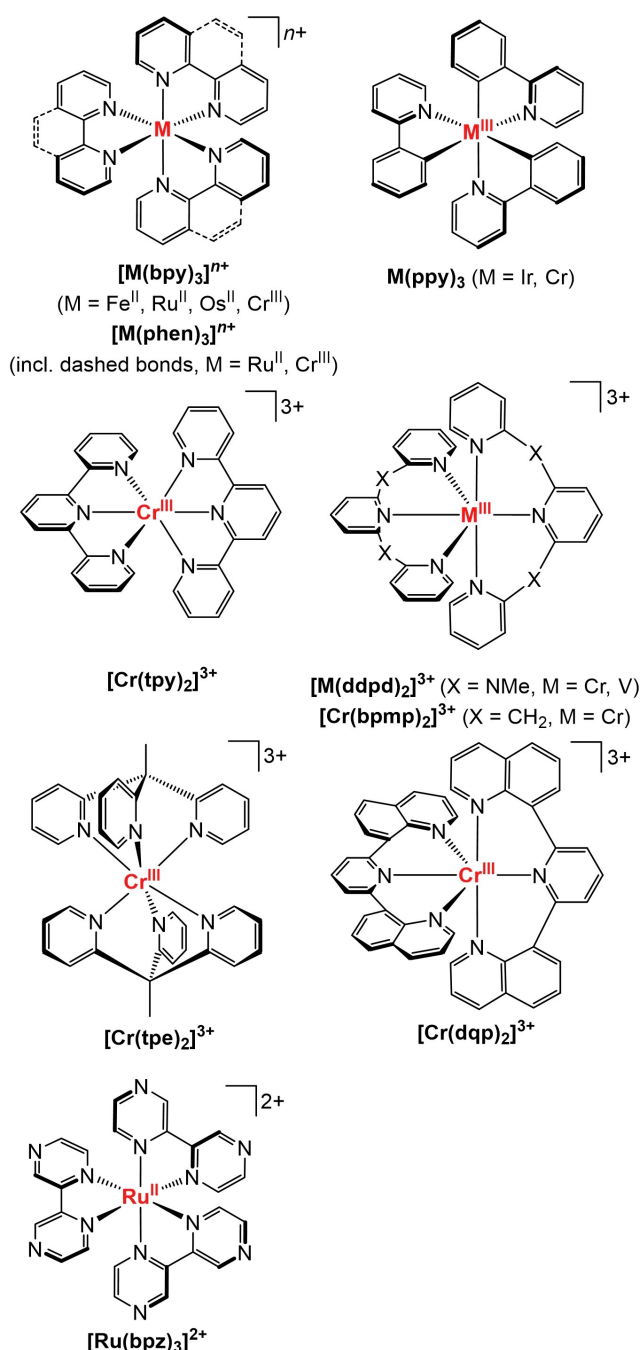
Winald R. Kitzmann studied chemistry at the University of Mainz, where he received his Bachelor's and Master's degree. Since 2020 he has been working on his PhD studies in the group of Prof. Dr. Katja Heinze as a fellow of the Max Planck Graduate Center and the German Academic Scholarship Foundation. He focuses on the synthesis and characterization of photoactive complexes using Earth-abundant metals. Currently, he is working on ultrafast polarized spectroscopy with Dr. Sascha Feldmann at the Rowland Institute at Harvard University as part of a research stay.

Katja Heinze received her PhD with Gottfried Huttner at the University of Heidelberg in 1998. After postdoctoral research at the University of Zurich, she set up her own research group. In 2008, she became full professor (W3) at the University of Mainz. She received the Elisabeth and Prof. Dr. Horst-Dietrich Hardt Award for her work on the photophysics of chromium(III) complexes in 2022. Since 2017, she has been coordinating the DFG priority program 2102 "Light-controlled reactivity of metal complexes".

$[M(bpy)_3]^{n+}$
(M = Fe^{II}, Ru^{II}, Os^{II}, Cr^{III})
$[M(phen)_3]^{n+}$
(incl. dashed bonds, M = Ru^{II}, Cr^{III})

M(ppy)$_3$ (M = Ir, Cr)

$[Cr(tpy)_2]^{3+}$

$[M(ddpd)_2]^{3+}$ (X = NMe, M = Cr, V)
$[Cr(bpmp)_2]^{3+}$ (X = CH$_2$, M = Cr)

$[Cr(tpe)_2]^{3+}$

$[Cr(dqp)_2]^{3+}$

$[Ru(bpz)_3]^{2+}$

Figure 2. Selected chemical structures of complexes discussed in this manuscript (bpy = 2,2′-bipyridine, phen = 1,10-phenanthroline, ppy⁻ = deprotonated 2-phenylpyridine, tpy = 2,2′:6′,2″-terpyridine, ddpd = N,N′-dimethyl-N,N′-dipyridin-2-yl-pyridine-2,6-diamine, bpmp = 2,6-bis(2-pyridylmethyl)pyridine, dqp = 2,6-bis(8′-quinolinyl)pyridine, tpe = 1,1,1-tris(pyrid-2-yl)ethane, bpz = 2,2′-bipyrazine).
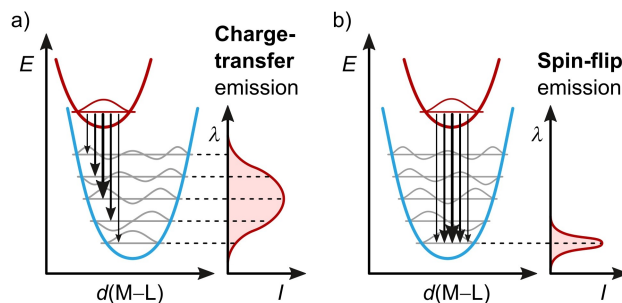
2.1. Charge-Transfer States

CT transitions involve the redistribution of charge within a molecule. The Coulomb attraction between the separated charges, the depopulation of (weakly) bonding orbitals, and the occupation of antibonding orbitals lead to a geometric

distortion of the CT state. In a simplified single configurational coordinate diagram, this can be understood as a horizontal displacement of the potential energy well (Figure 3a). The result is a strong vibronic coupling between the GS and the CT state as well as broad absorption and emission bands (strong coupling limit).[48] CT transitions are not restricted by parity rules and, thus, feature large transition dipole moments as well as high oscillator strengths, thereby resulting in large molar absorption coefficients ε in the range of 10^2 to 10^6 M^{-1}cm^{-1} and high radiative rates k_r.[80,81]

For comparison with SF emitters, it is interesting to note that CT luminescence can occur as fluorescence or phosphorescence. Although ISC to long-lived triplet excited states after initial spin-allowed excitation is very common, often ultrafast, and highly efficient in organometallic CT emitters, there are complexes that show CT fluorescence or thermally activated delayed fluorescence (TADF, see Section 3.2).[72,82–84] ISC is facilitated by the heavy atom effect by spin-orbit coupling (SOC) or vibronic coupling,[85] which also affects the radiative rates k_r of phosphorescence of typically 10^4 to 10^6 s^{-1}.[86]

For a detailed discussion, we take a look at $[Ru(bpy)_3]^{2+}$ and its photophysics as the prototypical CT chromophore with CT dynamics (Figures 1 and 4a). $[Ru(bpy)_3]^{2+}$ has a low-spin 4d^6 electron configuration $(t_{2g})^6$ with a singlet ground state (¹GS). Blue and green light excites the complex to its ¹MLCT states. Quantitative ISC to the ³MLCT states occurs within 15 ± 10 fs thanks to strong SOC.[88,91] During and after vibrational cooling (VC) within 300 fs,[88,92,93] the complex shows a broad phosphorescence, which reaches a maximum at 620 nm with a lifetime of 806 ns and an emission quantum yield of 9.5% in acetonitrile under deaerated conditions (Figure 5a, Table 1).[26,28,94]

Apart from the MLCT states, inter-configurational ³MC and ⁵MC states with electrons occupying M–L antibonding e_g^* orbitals can play an important role. Population of these ³MC/⁵MC states leads to large geometric distortions or even ligand dissociation and facilitates nonradiative deactivation of the ³MLCT states.[57,89,95,96] The MC energies are determined by the ligand-field splitting and the geometric distortion. Strong bpy ligands in combination with the large Ru^{II} ion place the energy of the relaxed ³MC states about

Figure 3. Single configurational coordinate ("potential well") diagrams with schematic emission spectra for a) charge-transfer emission with large excited-state distortion to a shorter M–L bond length and b) spin-flip emission with nested states.[48,62]
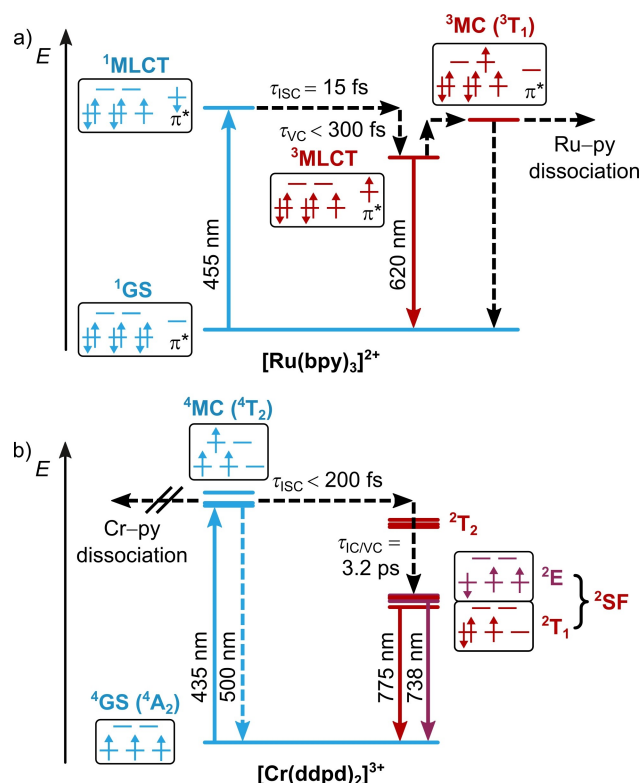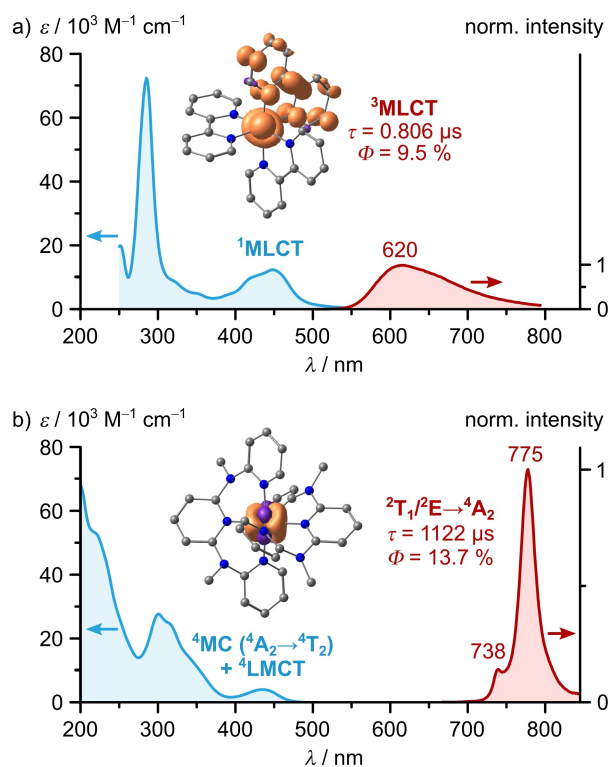
Figure 4. Jablonski diagrams of a) $[Ru(bpy)_3]^{2+}$ and b) $[Cr(ddpd)_2]^{3+}$ with experimental time constants for ultrafast processes (ISC = intersystem crossing, IC = internal conversion, VC = vibrational cooling, blue arrow = spin-allowed absorption, blue dashed arrow = fluorescence, red arrow = phosphorescence, black dashed arrow = nonradiative process).[41,61,87–89] The splitting of the (in octahedral symmetry degenerate) states in (b) was derived from CASSCF(7,12)-NEVPT2 calculations[90] and the relative energies of the different state sets were derived from experimental data.[61]

Figure 5. Absorption (blue trace) and luminescence spectra (red trace) of a) $[Ru(bpy)_3][PF_6]_2$ in deaerated acetonitrile solution and b) $[Cr-(ddpd)_2][BF_4]_3$ in deaerated aqueous solution at room temperature with molar absorption coefficients ε, emission lifetimes τ, emission quantum yields Φ, and spin densities of emissive states.[26,29,59–61,94] The emission spectra are scaled according to the respective emission quantum yields.[26,60] The spin densities of the respective a) lowest ^{3}MLCT (generated using Orca[97,98] from coordinates and parameters reported earlier)[89] and b) ^{2}E excited state[59] are shown at an isosurface value of 0.05 a.u. (orange = spin up, purple = spin down, gray = carbon, blue = nitrogen, hydrogen atoms omitted for clarity).

3600 cm^{-1} above the energy of the lowest ^{3}MLCT state.[87] In this case, thermally activated nonradiative relaxation via these ^{3}MC states is a relevant deactivation pathway for the ^{3}MLCT states at room temperature.[87] The ^{5}MC states in $[Ru(bpy)_3]^{2+}$ are at very high energy due to the large ligand-field splitting imposed by the 4d ion and consequently play no further role.[32]

As the 3d transition metal ions have a much lower intrinsic ligand-field splitting, CT states can efficiently relax nonradiatively via the low-energy ^{3}MC and ^{5}MC states.[32] For example, $[Fe(bpy)_3]^{2+}$ (Figure 2) is nonluminescent, as its ^{3}MLCT state evolves to the $^{3/5}$MC states within 50 fs and decays back to the ^{1}GS via the ^{5}MC state within 650 ps.[99,100] Only recently, ^{3}MLCT emissions with 3d^6 metals such as Cr^0, Mn^I, and Fe^{II} were achieved by using very strong ligands that raised the energy of the $^{3/5}$MC states sufficiently to prevent efficient depopulation of the ^{3}MLCT state, thereby allowing competitive phosphorescence and photocatalysis.[101–106]

A different strategy to avoid this problem entirely is using metal centers with a d^0 or d^{10} electronic configurations such as Ti^{IV}, Zr^{IV}, or Cu^I.[10,15,107–115] As a consequence of their full or empty d-shells, no excited MC states exist. For

linear Cu^I complexes, nonradiative deactivation of the LL′CT states could be shut down completely, thereby resulting in emission quantum yields of >99.9% in solution.[116]

2.2. Spin-Flip States

In contrast to CT states, SF transitions effect the smallest possible change in the electronic structure of a molecule: the flipping of a single electron spin. Since the electron

Table 1: Emission wavelengths λ_{em}, excited-state lifetimes τ, and phosphorescence quantum yields Φ of $[Ru(bpy)_3]^{2+}$ and $[Cr(ddpd)_2]^{3+}$ in acetonitrile (subscripts: Ar = deaerated solution, air = aerated solution).

	$[Ru(bpy)_3]^{2+}$	$[Cr(ddpd)_2]^{3+}$
λ_{em}/nm	620[29]	738, 775[59]
τ_{Ar}/µs (τ_{air}/µs)	0.806 (0.160)[94,117]	1122 (52)[60]
Φ_{Ar}/% (Φ_{air}/%)	9.5 (1.8)[26]	13.7 (0.8)[60]

configuration of the GS is preserved, no bonding orbitals are depopulated and no antibonding orbitals are occupied, SF states are only weakly distorted, and their potential wells are nested with the GS potential (weak coupling limit, Figure 3b). Therefore, SF emission bands are generally sharp (Figure 5).[49] Exceptions may occur when several individual SF transitions overlap[118] or when unsymmetric (ungerade) modes are activated in centrosymmetric complexes to enable the emission.[66,119]

SF transitions might bear some similarity to transitions observed in electron paramagnetic resonance (EPR) spectroscopy, as in both cases the relative orientation of unpaired electron spins is important. However, EPR probes transitions between states that mainly arise from differences in the orientation of the electron spins relative to an external magnetic field (different spin quantum number m_S),[120] whereas SF transitions occur between electronic states with a different orientation of the electron spins with respect to each other (different total spin S).

Transition dipole moments of MC transitions are generally small. Moreover, SF transitions are spin and Laporte forbidden, which is especially pronounced in centrosymmetric complexes. Consequently, radiative rates k_r are low (20–200 s^{-1}), leading to very long emission lifetimes of up to ms provided that the nonradiative rates are also low.[49,53,61,66]

The nature of SF states requires a spin change by $\Delta S = -1$ with respect to the GS (which obeys Hund's rule of maximum multiplicity) and thus an ISC process after the initial spin-allowed excitation to the Franck–Condon state.[49] Alternatively, SF states can be directly populated by energy-transfer (EnT) processes (see Sections 4.3 and 5).[121,122] The prime example is $^1O_2$, which is commonly sensitized by EnT[123,124] and shows a weak long-lived SF phosphorescence at 1275 nm from its lowest excited singlet state ($^1\Delta_g$) with two electrons paired in a π orbital.[125,126]

As a prototypical SF emitter, we selected [Cr(ddpd)$_2$]$^{3+}$, which has the nickname "molecular ruby". This chromium-(III) complex possesses a d^3 electron configuration, which gives a $^4A_2$ GS with three unpaired electrons occupying the t_{2g} orbitals (Figure 4b). The complex can be excited to the inter-configurational metal-centered $^4T_2$ state by irradiation at 435 nm.[59] Ultrafast ISC (< 200 fs) from vibrationally hot $^4T_2$ states to the intra-configurational doublet excited states is facilitated by a large density of $^2T_2$ states in this energy region. Vibrational cooling (VC) and internal conversion (IC) within 3.2 ps yield the two long-lived doublet SF states of $^2T_1$ and ^2E character.[61] Whereas the three electrons are evenly distributed in the t_{2g} orbitals in the ^2E state but with one spin flipped, two of the electrons are paired in the $^2T_1$ state (Figure 4b), so these states differ in orbital angular momentum. Please note that the orbitals and terms are given in the O notation, but in fact the D_2 symmetry of the complex splits the E and T terms into two and three states, respectively.[61] Interestingly, the electronic situation of the lowest doublet states of [Cr(ddpd)$_2$]$^{3+}$ is similar to that in singlet oxygen. The two singlet states in $^1O_2$, $^1\Delta_g$ and $^1\Sigma_g^+$, feature two electrons in π orbitals that are spin-paired in the same orbital or occupy different orbitals with antiparallel spin, respectively. However, the spin-paired $^1\Delta_g$ state is

markedly stabilized by its favorable orbital angular momentum.[126]

The molecular ruby shows a sharp dual phosphorescence reaching maxima at 738 and 775 nm with a common lifetime of 1.12 ms and a quantum yield of 13.7 % from the thermally equilibrated lowest $^2T_1$ and ^2E derived states in deaerated acetonitrile (Figure 5b, Table 1).[59,60] Residual fluorescence from the distorted $^4T_2$ states is very weak ($\Phi = 0.01$ %), in agreement with the fast ISC process.[61]

For a 3d^n metal complex ($n < 10$), the emission lifetime, quantum yield, as well as the photostability of [Cr(ddpd)$_2$]$^{3+}$ are exceptionally high and achieved by a large ligand-field splitting, which raises the energy of the $^4T_2$ states above the $^2T_1/^2E$ states in the Franck–Condon geometry. This large energy gap prevents thermally activated back-ISC occurring to the $^4T_2$ states followed by nonradiative deactivation, (delayed) fluorescence, or dissociation.[59,61,62]

3. Tuning of Excited-State Properties

3.1. Tuning of the Excited-State Energy

The simplest way to modulate the energy of CT states is by changing the (solvent) environment. As a result of their charge-separated nature, CT states are usually quite sensitive to the surrounding matrix (solvatochromism, see Section 4.3 for more details). Furthermore, the emission energy of CT emitters can be tuned by modifications of the complex changing the energy gap between the donating and accepting orbitals (Figure 6a).[31,127] In MLCT transitions, an electron is formally transferred from a d orbital to a ligand's π^* orbital, which results in an oxidized metal center and a ligand radical anion. Consequently, the excited state energy can be tuned by using a different metal center or by modifying the ligands.[31,128–130]

Changing the metal center of a complex results in different energies for the donating d orbitals. For example, using Os^{II} instead of Ru^{II} yields lower MLCT energies because of the higher energy of the 5d orbitals compared to the 4d orbitals (Figure 6a).[128]

In principle, it is expected that the energy of an MLCT state will decrease on introducing electron-withdrawing substituents that lower the accepting π^* orbital energy and will increase with electron-donating substituents that raise the π^* orbital energy. However, ligand modifications also affect the energy of the d orbitals. For example, an electron-donating substituent also increases the energy of the metal's d orbitals in addition to destabilizing the ligands' π^* orbitals.[128] Introducing two diethylamino substituents onto the bpy ligands red-shifts the emission band to 700 nm for the homoleptic ruthenium(II) complex because the destabilizing effect on the d orbitals is stronger than on the π^* orbitals, thereby leading to a lower energy gap between the two levels.[131]

As a consequence of this intricate interplay between the ligand and metal center outlined above, careful control of the donating and accepting orbital energies is needed to achieve MLCT emission in the near-infrared (NIR) spectral
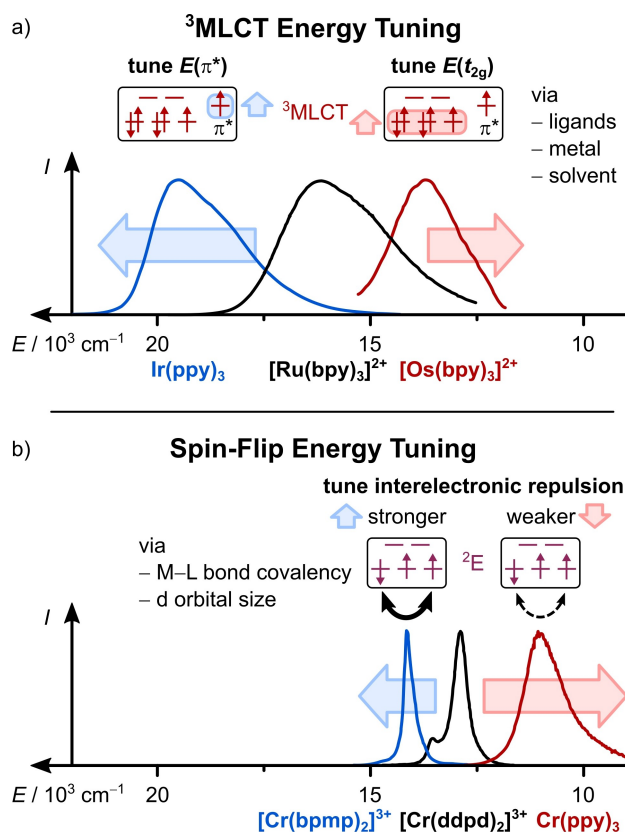
Figure 6. Strategies for tuning the emission energy as illustrated using normalized emission spectra of key examples of a) ^{3}MLCT emitters and b) SF emitters (ppy$^-$ = anion of 2-phenylpyridine, bpmp = 2,6-bis(2-pyridylmethyl)pyridine, Figure 2).[29,61,63,138–140]

region. For example, a combination of electron-rich ligands to destabilize the d orbitals and an electron-poor ligand to provide a low-energy π^* accepting orbital enabled NIR phosphorescence to be achieved.[128] Other designs include extended aromatic systems on the ligands and polynuclear complexes, amongst others.[129,130,132–134] In any case, the low-energy excited states required for NIR emission suffer from enhanced rates of nonradiative deactivation according to the energy gap law, which negatively impacts lifetimes and quantum yields.[135] In contrast, efficient green or even blue emission from CT states is readily achieved, for example from complexes derived from Ir(ppy)$_3$ (Figure 6a).[25,136,137]

The typical spectral range for SF emission is deep-red to NIR-I (780–1000 nm) or even NIR-II (1000–1700 nm).[49] No charge separation and no (or only a slight) change in orbital occupation occurs in SF transitions. Instead, the energy of SF states results from additional repulsive interactions between the electrons in nearly degenerate orbitals caused by a lower exchange energy, which are often quantified with the Racah parameters B and C derived from ligand-field theory.[64,81,141,142] Hence, strategies for tuning emission energy are less obvious than in the CT case.[49]

Successful strategies are changing the covalency of the metal–ligand bonds and varying the size of the d orbitals. More covalent M–L bonds lower the energies of the SF state

because the interelectronic repulsion is reduced by delocalization of the electrons onto the ligands (nephelauxetic effect). This principle was demonstrated with Cr^{III} complexes containing carbanionic ligands such as ppy$^-$ (Figure 6b) or amido ligands leading to NIR emission band maxima up to 1067 nm.[139,142,143]

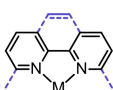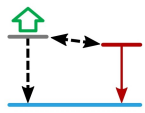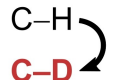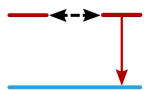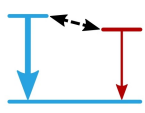More ionic M–L bonds result in higher emission energies, but this is difficult to achieve in molecular systems. Recently, [Cr(bpmp)$_2$]$^{3+}$ (Figure 2, bpmp = 2,6-bis(2-pyridylmethyl)pyridine) was reported, which emits at 709 nm (1.75 eV) with a high quantum yield of 19.6 % and a millisecond lifetime. The ligand design was guided by high-level quantum mechanical calculations.[63]

The central metal ion profoundly affects the energy of the SF state. Metal centers with larger d orbitals (lower effective charge, higher period) reduce the interelectronic repulsion and hence the SF state energy, while those with small d orbitals (higher effective charge, lower period) increase the SF energy.[49] For example, the Racah parameter B of the free ions qualitatively predicts that V^{III} [B(V^{3+}) = 861 cm^{-1}] and Mo^{III} complexes [B(Mo^{3+}) = 610 cm^{-1}] should possess lower energy SF states than Cr^{III} complexes [B(Cr^{3+}) = 918 cm^{-1}] in similar environments and assuming a similar ratio C/B.[49,81] In fact, [V(ddpd)$_2$]$^{3+}$ (Figure 2) and MoCl$_3$(urea)$_3$ emit between 982–1109 nm[72] and at 1095 nm,[144] respectively, while the emission from Cr^{III} complexes is usually located between 720 and 800 nm.[48,49,53,58] We would like to point out that the Racah parameters B and C should be used with caution for quantitative comparisons, as the assumptions in the underlying ligand-field theory (ligands treated as point charges, ideal coordination geometries)[81] might not be valid, especially for complexes with low symmetry and highly anisotropic bonding situations.

In contrast to CT emitters, it is challenging to blue-shift SF emission by varying the metal center. One problem is that ions in high oxidation states such as Mn^{IV} with contracted d orbitals can form highly covalent M–L bonds, eventually leading to low-energy SF states.[78] Additionally, very high or low oxidation states of the metal center can also introduce low-energy CT states, which can facilitate nonradiative deactivation, for example through mixing with the luminescent SF states.[49,78,145]

3.2. Tuning the Emission Lifetime

Control over the luminescence lifetime τ is crucial, as requirements vary depending on the application. For example, a long lifetime is generally desirable for photocatalysts, because it increases the quenching efficiency.[146] In contrast, shorter lifetimes arising from higher radiative rates k_r are preferred for chromophores in organic light-emitting diodes (OLEDs) to limit photodegradation and maximize performance.[147] A variety of strategies exist to influence the lifetime τ through the radiative and nonradiative rates k_r and k_{nr} [Eq. (1), Figure 7].[148]

	Charge-Transfer Emitters	Spin-Flip Emitters

Figure 7. Strategies for tuning the emission lifetime in CT and SF emitters (see main text for details). Check mark = examples are published, cross = not applicable, dash = possible but not advantageous. TADF = thermally activated delayed fluorescence.

$$\tau = 1/(k_r + k_{nr}) \qquad (1)$$

An efficient way of prolonging τ is rigidification of the ligand scaffold (Figure 7). This can decrease k_{nr} through the restriction of intramolecular motions in the excited state. This strategy succeeded for CT, SF, and organic emitters alike.[62,148–150] For example, the phen complexes of Ru[II] and Cr[III] (Figure 2) have emission lifetimes that are longer by factors of about 1.5 and 4, respectively, compared to their bpy analogues.[31,55] Furthermore, Cr[III] complexes with tris(bidentate) chelation such as [Cr(bpy)₃]³⁺ show a trigonal distortion in the excited state that facilitates nonradiative deactivation of the SF states.[151,152] This mode can be shut down by employing tridentate ligands, such as in [Cr(ddpd)₂]³⁺.[62]
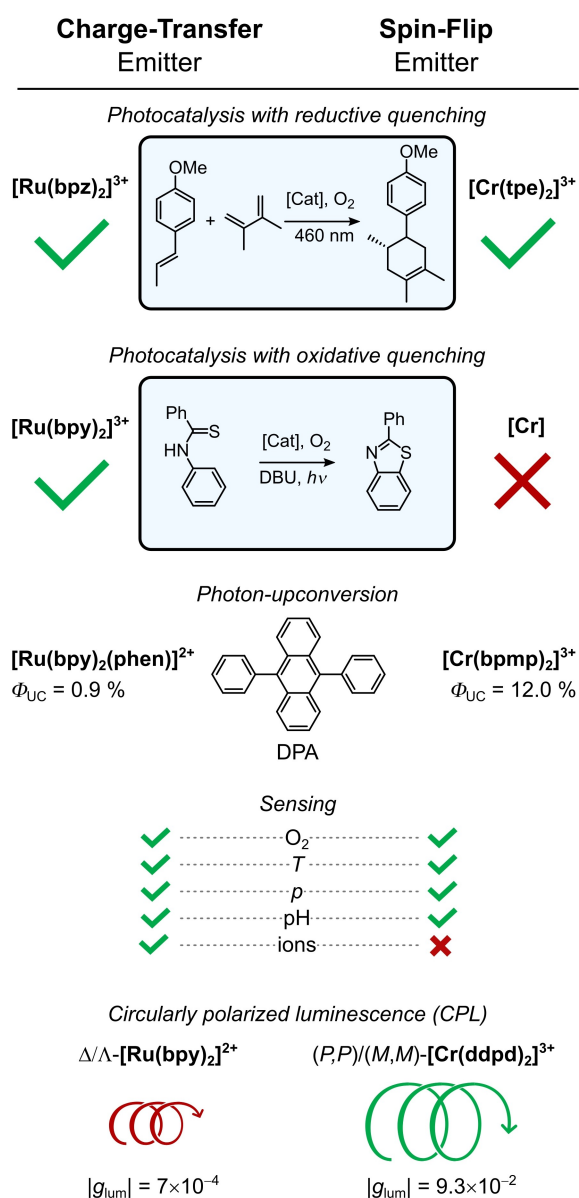
In CT states, the geometric distortion can be reduced by stronger delocalization of the excited state on an extended π-system of the ligand (Figure 7).[102,148] This diminishes the impact of the charge separation on individual bonds and, thus, coupling to the GS. In SF emitters, a delocalization of the excited state, for example by mixing with CT states, has the contrary effect: it increases the geometric distortion and facilitates nonradiative deactivation.[78,142,145]

Lifetimes of Ru[II] complexes were prolonged by a larger ³MLCT-³MC energy gap limiting nonradiative decay via the detrimental ³MC states (Figure 7). For example, a larger bite-angle of the chelating ligand raises the ligand-field splitting and, thus, the ³MC energy, while electron-withdrawing substituents on the ligands lower the ³MLCT states.[153] Similarly, increasing the energy of the ⁴T₂ MC states in [Cr(ddpd)₂]³⁺ proved to be key to its remarkable optical properties, as it prevents deactivation of the SF states via back-ISC.[59,61,62]

Deuteration of the ligands or solvents is a particularly useful strategy that lowers k_{nr} for low-energy luminescence of any kind (Figure 7).[154,155] Above an emission wavelength of about 700 nm (< 14300 cm⁻¹), the energy of the electronically excited state is in the region of X–H (X = C, N, O, 3000–3500 cm⁻¹) overtone vibrations of the ligand or solvent, and deactivation through energy transfer becomes relevant. This process requires a spectral overlap between the emission band of the complex and the overtone absorption band. Deuteration mitigates the negative effect of these oscillators, as X–D vibrations are significantly lower in energy than their X–H counterparts [$\tilde{\nu}$ (C–H) ≈ 3000 cm⁻¹, $\tilde{\nu}$(C–D) ≈ 2200 cm⁻¹], thus requiring a higher overtone to match the emission energy. The lower molar absorption coefficient of the higher overtone leads to a smaller spectral overlap and reduced deactivation. For the molecular ruby, statistical deuteration of the ddpd ligand increases the emission lifetime from 1.12 to 2.3 ms and the quantum yield from 13.7 to 30 %.[156] Since the rate of energy transfer strongly decreases with the M···X–H distance ($\approx r^{-6}$), the α–C–H oscillators are the most important ones. Hence, deuteration of the α–C–H groups of the bpmp ligands in [Cr(bpmp)₂]³⁺ (Figure 2) boosts the lifetime from 1.8 to 2.5 ms and the quantum yield from 19.6 to 24.6 %.[63] Similarly, but to a lesser extent, perdeuteration of [Ru(bpy)₃]²⁺ increases the emission lifetime by about 20 % in aqueous solution.[157] The smaller effect arises from the higher emission energy of [Ru(bpy)₃]²⁺.

The lifetime of CT emitters such as [Ru(bpy)₃]²⁺ can be increased by exploiting the so-called reservoir effect (Figure 7). The ligands are decorated with aryl substituents, such as pyrene, that possess similar triplet energies as the parent complex.[146,158–162] After photoexcitation and ISC, a thermal equilibrium between the ³MLCT state and the pyrene-based ³(π-π*) state is established through an intramolecular energy transfer. The very long-lived pyrene triplet state ($\tau = 9.4$ ms in ethanol)[163] serves as a reservoir that slowly repopulates the emissive ³MLCT state and leads to microsecond emission lifetimes.[161] Adding 9,10-diphenylanthracene (DPA, Figure 8) to a solution of [Cr(bpmp)₂]³⁺ (Figure 2) also prolongs the lifetime through a doublet-triplet energy-

Charge-Transfer Emitter		Spin-Flip Emitter

Photocatalysis with reductive quenching

[Ru(bpz)$_2$]$^{3+}$

[Cr(tpe)$_2$]$^{3+}$

✓ ✓

Photocatalysis with oxidative quenching

[Ru(bpy)$_2$]$^{3+}$

[Cr]

✓ ✗

Photon-upconversion

[Ru(bpy)$_2$(phen)]$^{2+}$
Φ_{UC} = 0.9 %

[Cr(bpmp)$_2$]$^{3+}$
Φ_{UC} = 12.0 %

DPA

Sensing

✓	·········· O$_2$ ··········	✓
✓	·········· T ··········	✓
✓	·········· p ··········	✓
✓	·········· pH ··········	✓
✓	·········· ions ··········	✗

Circularly polarized luminescence (CPL)

Δ/Λ-[Ru(bpy)$_2$]$^{2+}$ (P,P)/(M,M)-[Cr(ddpd)$_2$]$^{3+}$

|g_{lum}| = 7×10^{-4} |g_{lum}| = 9.3×10^{-2}

Figure 8. Selection of applications for complexes with CT and SF excited states (see main text for details).[69, 164, 235–239] Tick = examples are published, cross = not reported. bpz = 2,2′-bipyrazine, tpe = 1,1,1-tris(pyrid-2-yl)ethane, bpy = 2,2′-bipyridine, phen = 1,10-phenanthroline, DBU = 1,8-diazabicyclo[5.4.0]undec-7-en, bpmp = 2,6-bis(2-pyridylmethyl)pyridine, ddpd = N,N′-dimethyl-N,N′-dipyridin-2-yl-pyridine-2,6-diamine (Figure 2).

transfer equilibrium between the SF states and triplet state of DPA. However, unlike the CT emitters, the lifetime was not increased beyond the value of 1.8 ms found for the complex without additives.[164] As excited-state lifetimes are already very long, this also seems unnecessary as a molecular design strategy for SF emitters.

As a consequence of the spin-forbidden nature of phosphorescence transitions, the possibilities to increase their radiative rates include increasing the metal character of the involved wavefunctions (e.g. by changing the character of the lowest state from LL′CT to MLCT),[165] installing

heavy atoms to increase spin-orbit coupling (SOC)[166,167] and to increase the density of states which can interact with the emissive state through SOC, for example, by a multi-metal approach.[168] Another strategy that was thoroughly explored for CT emitters is thermally activated delayed fluorescence (TADF, Figure 7).[84,109,169–173] Here, an emissive triplet state is in thermal equilibrium with an energetically higher lying singlet state ($\Delta E_{ST} < 1600$ cm^{-1})[174,175] through back-ISC. The repopulated singlet state decays through fluorescence to the ^{1}GS with a high radiative rate, as no change in multiplicity is involved.

For Cr^{III} complexes as prototypical SF emitters, TADF occurs in cases where back-ISC from the ^{2}E/^{2}T$_1$ states to the ^{4}T$_2$ state is thermodynamically possible.[56] However, apart from fluorescence, other deactivation pathways of the ^{4}T$_2$ state, such as ligand dissociation and surface crossing, are available due to the strong Jahn–Teller distortion of the ^{4}T$_2$ state.[176,177] Hence, enabling back-ISC in Cr^{III} complexes comes at the cost of poor quantum yields, as discussed above. Therefore, TADF cannot be considered a viable strategy to tune SF emitters, at least with the chromium(III) complexes developed so far.

The metal-confined nature of the SF states enables tuning of the radiative rate constant k_r by exploiting Laporte's rule (Figure 7).[119] By introducing an inversion center in [Cr(tpe)$_2$]$^{3+}$ using the tripodal ligand tpe (=1,1,1-tris(pyrid-2-yl)ethane, Figure 2), the radiative rate of the spin- and Laporte-forbidden ^{2}E$_g$/^{2}T$_{1g}$→^{4}A$_{2g}$ transitions was lowered to merely $k_r = 18$ s^{-1}, thereby resulting in a record luminescence lifetime of 4.5 ms.[66] This strategy is not available for CT emitters, since the charge separation does not occur in orbitals of the same parity and always leads to symmetry breaking.

4. External Effects

4.1. Temperature

Some of the effects of temperature on the ^{3}CT and SF luminescence, such as thermal deactivation via MC states and TADF, have been discussed in the previous sections.

Equilibria can also exist between phosphorescent states of different character. For example, temperature-dependent dual emission arises from an excited-state equilibrium between a ^{3}MLCT and a ligand-centered ^{3}LC state in an [Ir(ppy)$_2$(N^N)]$^+$ complex featuring a pyrimidyltriazole ligand (N^N).[165]

In SF emitters such as the molecular ruby, temperature-dependent changes in the number of emission bands and their shape are largely governed by the population of close-lying SF states that arise from the splitting of SF states degenerate in an ideal octahedral symmetry (^{2}E, ^{2}T$_2$, Figure 4b). As the energy gaps amount to around 200–800 cm^{-1} with small barriers, the population follows a Boltzmann distribution.[48,49,63,64,178] Hence, the molecular ruby has been used as a self-referencing ratiometric optical thermometer.[178,179] The three ^{3}MLCT states in derivatives

of $[Ru(phen)_3]^{2+}$ (Figure 2) are also split in D_3 symmetry, but only by about 10 and 60 cm^{-1}.[31,180]

Although the population of the close-lying SF states varies with temperature, the energies of the individual states generally remain unaffected in most cases[64,66,178] with rare exceptions.[73] In contrast, drastic changes in the emission energy and band shape can be observed for CT emitters upon freezing of the solution. This phenomenon, known as rigidochromism, will be discussed in more detail in Section 4.3 as it is not primarily a temperature effect.

4.2. Pressure

Pressure can increase the excited-state lifetimes and photo-luminescence quantum yields of some CT and SF emitters. This can be explained by a stronger interaction between the metal center and the ligands under pressure, which increases the ligand-field splitting and thus the energy of deactivating MC states.[95,181,182] For $[NH_4]_3[CrF_6]$ in the solid state, this effect even causes a change in the emission type: at low pressures the complex fluoresces weakly from the inter-configurational $^4T_2$ MC state, while SF phosphorescence occurs at pressures above 71 kbar.[183] In $[Ru(bpy)_3]^{2+}$, the pressure response of the luminescence intensity is strongly dependent on the environment. While the emission quantum yield increases in acetonitrile solution and doped solids, a decrease in Φ was found in single crystals.[95,181,184,185] High pressures can restrict vibrational modes and limit non-radiative deactivation, as shown for $[Ru(bpy)_2(py)_2]^{2+}$ with the more flexible pyridine ligands (py).[186,187]

Hydrostatic pressure can also affect the energy of the SF emission. The most well-known example is the shift of about -0.8 cm^{-1}kbar^{-1} of the SF emission from the gemstone ruby (Al_2O_3:Cr^{3+}), which is exploited for optical measurements of high pressures in diamond anvil cells.[188,189] Much stronger shifts of up to -14.8 cm^{-1}kbar^{-1} are found in the molecular ruby $[Cr(ddpd)_2]^{3+}$ in solution and the solid state.[90] This pressure effect on the SF emission is caused by subtle changes in the coordination geometry and the π(M–L) overlap affecting the M–L covalency and the nephelauxetic effect.[90]

For CT emitters, the effect is usually less pronounced. The emission energy of $[Ru(bpy)_3]^{2+}$ shows red-shifts of -2 to -6 cm^{-1}kbar^{-1} depending on the matrix and pressure range.[95,184,187] For some CT emitters, the shift can be traced back to pressure-induced changes of solvent parameters (see Section 4.3).[190] A strong shift of -13 cm^{-1}kbar^{-1} was found in single crystals of a heteroleptic ruthenium(II) complex, which was ascribed to a pressure-dependent hydrogen bonding of the complex to a salt bridge.[191]

4.3. Environment

The influence of the solvent on the emission properties is very much tied to the nature of the excited states involved. CT transitions are more sensitive to changes in the environment because of their large change in the dipole moment.[192]

SF states only show a minimal electron redistribution with respect to the GS. Here, effects of the matrix are limited to changes in the emission quantum yields and lifetimes,[49] whereas for CT states the energy can strongly vary with solvent parameters.[193–197] If the excited state has a lower dipole moment than the GS, the emissive state is destabilized in more polar solvents, which leads to a higher emission energy (negative solvatochromism). Excited states that are more polar than the GS show a red-shift in more polar solvents (positive solvatochromism).[198,199] For example, the positive solvatochromism of $[Ru(bpy)_2(CN)_2]^+$ enables tuning of the emission energy in the range of 623 to 712 nm.[200]

Apart from solvent, charged complexes can also be affected by interactions with their counterions. For example, variations in ion pairing can open different reaction pathways.[201,202] With regards to luminescence, strong effects have been observed for CT emitters.[203–205] The emission quantum yield of an iridium(III) ^{3}MLCT emitter in the solid state could be increased 12-fold by employing bulky counterions. The effect was rationalized by a larger average distance between the complex molecules leading to reduced self-quenching.[206]

In the molecular ruby, counterions and the solvent influence the emission lifetime and quantum yield, but not the ultrafast ISC and internal conversion (IC) processes after excitation.[60,156] For $[Cr(bpy)_3]^{3+}$, it was shown that the counterions and co-solutes help to rigidify the ligand scaffold and reduce nonradiative decay.[207]

In general, phosphorescence can be quenched by $^3O_2$ through a Dexter energy transfer (EnT) which leads to the formation of $^1O_2$ and significantly reduced excited-state lifetimes (Table 1).[123,208,209] $^1O_2$ can be a useful reagent, for example, for the α-cyanation of amines[210,211] or photo-dynamic therapy,[212,213] but in some cases quenching by O_2 is undesired.[214] In principle, steric shielding can help to limit the EnT process, as it requires orbital overlap between the energy donor and energy acceptor. For CT emitters with spatially extended excited states, however, such a steric protection is challenging due to large delocalization of the ^{3}MLCT wavefunction onto the ligands.[214] The SF states in the molecular ruby, on the other hand, can be efficiently protected from external influence by shielding the metal center.[215]

A phenomenon that can be found in CT emitters is rigidochromism. It describes the blue-shift of the emission band upon rigidification of the environment.[192,216] Although it can occur during freezing of a solution, rigidochromism is not a temperature effect, as similar shifts can be observed when comparing the emission spectra recorded in a frozen solution and in the solid state at room temperature. For example, the emission of $[Ru(bpy)_3]^{2+}$ shifts from 601 nm at room temperature[217] to 580 nm in a frozen diethyl ether:i-isopentane:ethanol solution at 77 K[218] as well as in the solid state at room temperature.[219]

5. Applications

When choosing transition metal complexes for an application it is crucial to consider their ground- and excited-state properties, as they have important implications for different scenarios.

One of the most common applications of photoactive complexes is photoredox catalysis, which exploits a photoexcited complex having a stronger oxidative and reductive power than the GS.

Hence photoexcited complexes can be used to drive redox reactions under mild conditions with high selectivity.[6] The excited-state redox potentials E^* for an electron donor D or electron acceptor A can be estimated from the redox potentials E of the GS and the energy of the excited state E_{00} using the modified Rehm–Weller equations [Eqs. (2) and (3), respectively], where e is the elementary charge and the work term for the charge separation is omitted.[220–223]

$$E^*(D^+/D^*) = E(D^+/D) - E_{00}/e \qquad (2)$$

$$E^*(A^*/A^-) = E(A/A^-) + E_{00}/e \qquad (3)$$

A common rationalization for the stronger redox powers of excited states has been that the charge separation, for example in MLCT states, results in an electron hole that is easier to fill and an electron radical in a π^* orbital that is easier to remove.[6,29,223] In fact, there is a plethora of complexes of various metal centers such as Ru^{II}, Ir^{III}, Mo^0, Zr^{IV}, W^{VI} or Cu^I with ^{3}CT states that have been used as oxidative and reductive photocatalysts and have supported the explanation given above.[6–8,10,28,107,224–226]

Interestingly, Cr^{III} complexes can also be applied in photoredox reactions and catalysis even though they lack charge separation in their SF states.[69,223,227–231] Most recently, [Cr(tpe)$_2$]$^{3+}$ was applied for a light-induced radical cation [4+2] cycloaddition (Figures 2 and 8), and [Cr(dqp)$_2$]$^{3+}$ (dqp = 2,6-bis(8′-quinolinyl)pyridine, Figure 2) catalyzed a variety of transformations such as bromination, oxygenation, hydroxylation, and vinylation reactions.[69,223] Importantly, the excited-state reduction potential of [Cr(dqp)$_2$]$^{3+}$ can be estimated in the same way as for ^{3}MLCT states for photoinduced electron transfer [Eq. (3)], despite lacking any charge separation.[223] Possibly the simplistic orbital picture with holes and electrons that has served as an explanation needs to be replaced with a model that focuses more on excited electronic states instead.[223]

One advantage of Cr^{III} catalysts of the molecular ruby type over traditional Ru^{II} catalysts is their remarkable photostability. [Cr(tpe)$_2$]$^{3+}$ is stable under catalytic conditions for a Diels–Alder reaction and can be re-used, whereas [Ru(bpz)$_3$]$^{2+}$ (bpz = 2,2′-bipyrazine, Figure 2) decomposes after 30 min under the applied conditions. Similarly, under anaerobic conditions, the photodecomposition quantum yield Φ_{degr} of [Cr(dqp)$_2$]$^{3+}$ (Figure 2) is very low (0.0019%) and comparable to that of Ir(ppy)$_3$, whereas no degradation was observed when irradiating in the presence of O$_2$.[223,232] The ligand-centered reduction of [Cr(tpe)$_2$]$^{3+}$ and [Cr(dqp)$_2$]$^{3+}$ in photocatalysis[69,223] is beneficial for stability, as

it prevents the formation of genuine chromium(II) complexes that are prone to follow-up reactions, as exemplified by [Cr(ddpd)$_2$]$^{2+}$.[233,234]

One of the more fundamental differences between Cr^{III} and Ru^{II} complexes lies in the multiplicity of their photoexcited states (doublet vs. triplet). As a consequence, the radical pairs formed after photoinduced electron transfer can have different total spins depending on the catalyst. It was suggested that this might affect the recombination dynamics and cage escape yields of the radical pairs.[223] Furthermore, the charges of the Cr^{III} and Ru^{II} photocatalysts differ, which might also affect the cage escape yields. However, more data is required to allow for a generalized conclusion.

Unlike many precious metal complexes, the application of Cr^{III} complexes in photoredox catalysis is currently limited to mechanisms involving reductive quenching of the excited state (Figure 8).[69,223,240,241] Transformations driven by oxidative quenching of molecular Cr^{III} catalysts have not yet been reported. This is possibly due to the difficulty in accessing a reversible Cr^{III}→Cr^{IV} oxidation[59] and not because of an intrinsic limitation of SF states in this regard, as oxidative quenching of doublet SF states has been observed in Mo^{III} complexes.[74]

CT and SF excited states can also be quenched by energy-transfer (EnT) pathways.[44,66,122,164,242,243] The most common example is the quenching of phosphorescence by ^{3}O$_2$ to form ^{1}O$_2$ through a Dexter-type energy-transfer process (see Section 4.3). With substituted acceptors such as DPA (Figure 8), green-to-blue photon upconversion processes involving triplet-triplet annihilation (TTA) of ^{3}DPA become feasible.[244,245] [Ru(bpy)$_3$]$^{2+}$ in the ^{3}MLCT state undergoes triplet-triplet EnT to form ^{3}DPA, while [Cr(bpmp)$_2$]$^{3+}$ in its ^{2}T$_1$/^{2}E states shows doublet-triplet EnT to DPA.[164] Although this difference in excited state multiplicities affects some details of the process, the overall mechanism of the TTA upconversion remains the same in both cases.[164] The system [Cr(bpmp)$_2$]$^{3+}$/DPA reached an upconversion quantum yield Φ_{UC} of 12.0%, which is close to the theoretical maximum,[164] whereas [Ru(bpy)$_2$(phen)]$^{2+}$/DPA only gave a Φ_{UC} of 0.9% because of the much shorter ^{3}MLCT lifetime (Figure 8).[236] Less-substituted anthracenes can undergo a [4+4] cycloaddition to give anthracene dimers using green light instead of the required UV-blue light without a sensitizer.[164,246]

In general, the metal-confined nature of the SF states represents a downside for electron transfer and EnT processes, as low orbital overlap with substrates may limit the quenching efficiency.[44] In contrast, CT states extend over large parts of the molecule and are also delocalized onto the periphery of ligands, thereby ensuring sufficient overlap with substrate orbitals. Cr^{III} complexes may partially compensate this disadvantage with their very long excited-state lifetimes of µs to ms.[44,69,223]

By means of clever ligand design, CT and SF emitters have been successfully employed for a variety of sensing applications (Figure 8): The introduction of acidic or basic groups on the ligands enabled pH sensing,[63,67,247–250] O$_2$ sensing was achieved by exploiting the quenching of

phosphorescence by $^3O_2$, with the formation of $^1O_2$,[179,251] and a variety of mechanisms such as TADF, close-lying thermalized SF states, and thermally activated nonradiative decay can enable temperature sensing (see Sections 3.2 and 4.1).[252] At this point we want to highlight that the large spatial extent of CT states can lead to specific interactions with ions in solution, thus enabling optical ion sensing.[253,254] SF emitters, on the other hand, are more suitable as hydrostatic pressure sensors in solution as a consequence of the uniquely large pressure response of their emission energy (see Section 4.2).[90]

Chiral luminophores can show circularly polarized luminescence (CPL), which holds great promise for applications such as security inks, polarized microscopy, and display technology.[238,255–263] CPL is commonly quantified using the dissymmetry factor g_{lum}, which describes the excess of left-handed circularly polarized light over right-handed CPL [Eq. (4), $-2 \leq g_{lum} \leq 2$].[238,264] The theoretical description of the dissymmetry factor reveals that a high value can be expected for electronic transitions that are spin-forbidden (low electronic transition dipole moment $|\vec{\mu}_{ba}|$) and magnetically allowed [high magnetic transition dipole moment $|\vec{m}_{ab}|$, Eq. (4)]; τ_{ab} is the angle between the two vectors.[264]

$$g_{lum} = (I_L - I_R)/[0.5(I_L + I_R)] \approx 4|\vec{m}_{ab}|\cos\tau_{ab}/|\vec{\mu}_{ba}| \qquad (4)$$

These selection rules are very favorable for SF emitters, and result in g_{lum} values up to 0.20,[64,65,239,265,266] whereas CT emitters typically have values below 0.005.[238,260,267,268] The Δ and Λ enantiomers of $[Ru(bpy)_3]^{2+}$ show only weak CPL, with $|g_{lum}| = 0.0007$ at 625 nm (Figure 8).[237,238] In $[Cr(ddpd)_2]^{3+}$, the tridentate ligands coordinate the metal ion forming a double helix which generates (P,P) and (M,M) enantiomers. After separation of the enantiomers by HPLC on chiral stationary phases, a high luminescence dissymmetry factor $|g_{lum}|$ of 0.093 was obtained for the emission at 775 nm.[239] Enantiomerically pure substituted $[Cr(dqp)_2]^{3+}$ complexes can even achieve $|g_{lum}| = 0.17$–0.20.[64,65]

6. Summary and Outlook

Charge-transfer emitters have been at the center of photochemical and photophysical research for decades. The tunability of their ground- and excited-state properties over a wide range made them versatile assets for a variety of applications. Over the past years, the dominance of charge-transfer emitters based on precious metal ions such as Ru^{II}, Re^I, Os^{II}, or Ir^{III} in the scientific literature has been challenged by other metal centers, including many base metals. By means of creative ligand design, more and more reports feature photoactive 3d and Earth-abundant 4d metal complexes.[1,4,5,78,103,106,269–277] In the midst of this shift in focus, there has been a revival of Cr^{III} complexes with long-lived excited states and strong spin-flip emission.[53,59,61,63–67,139,142,278,279]

In some regards, spin-flip luminescence can be considered complementary to its charge-transfer counterpart. The most apparent difference is the localization of spin-flip states

on the metal center with no change in orbital occupation compared to the ground state, whereas charge-transfer transitions can be considered as intramolecular redox reactions that can spread over large parts of the molecule. With this fundamental distinction in mind, it is possible to understand the differences between charge-transfer and spin-flip emitters with respect to bandwidths (broad vs. sharp), photostability (low vs. high), photoelectron transfer efficiency (high vs. moderate), emission lifetimes (short vs. long), matrix effects (strong vs. weak), and circularly polarized luminescence efficiency (low vs. high) amongst others.

Furthermore, typical charge-transfer and spin-flip state energies cover complementary spectral regions. Although the energy of charge-transfer states is readily tuned over the full visible spectrum, low-energy emission in the near-infrared is challenging to achieve. In contrast, spin-flip phosphorescence is commonly found in the deep-red to near-infrared spectral region. Tuning the emission energy, especially blue-shifting, is not straightforward and, hence, spin-flip energies above 1.85 eV (670 nm) have yet to be reported.[48,49,53]

It is also worth noting where charge-transfer and spin-flip states behave similarly: Both can be used successfully in energy-transfer reactions. Importantly, spin-flip states can also drive photoredox catalytic reactions, which had long been thought to be a unique feature of charge-separated states. In fact, Cr^{III} complexes with their very long excited-state lifetimes and high photostability are attractive photocatalysts, since they also employ an Earth-abundant metal. However, there are still some practical limitations, such as the lack of redox stability to support transformations requiring oxidative quenching. Research in this field has just begun, after much effort was spent on understanding the fundamental properties of the new class of highly luminescent chromium(III) complexes.[59,62–65,139,142,178,210,279–281]

With the paradigm change from merely parasitic metal-centered excited states to well-performing spin-flip excited state, it is anticipated that spin-flip emitters will join their charge-transfer relatives in a versatile toolbox and drive scientific research beyond the boundaries of individual academic fields.

Acknowledgements

Conflict of Interest

The authors declare no conflict of interest.

[1] C. Wegeberg, O. S. Wenger, *JACS Au* **2021**, *1*, 1860–1876.

[2] P.-T. Chou, Y. Chi, M.-W. Chung, C.-C. Lin, *Coord. Chem. Rev.* **2011**, *255*, 2653–2665.

[3] J. K. McCusker, *Science* **2019**, *363*, 484–488.

[4] C. Förster, K. Heinze, *Chem. Soc. Rev.* **2020**, *49*, 1057–1070.

[5] O. S. Wenger, *J. Am. Chem. Soc.* **2018**, *140*, 13522–13533.

[6] C. K. Prier, D. A. Rankic, D. W. C. MacMillan, *Chem. Rev.* **2013**, *113*, 5322–5363.

[7] J. Twilton, C. Le, P. Zhang, M. H. Shaw, R. W. Evans, D. W. C. MacMillan, *Nat. Chem. Rev.* **2017**, *1*, 0052.

[8] *Visible Light Photocatalysis in Organic Chemistry* (Eds.: C. Stephenson, T. Yoon, D. W. C. MacMillan), Wiley-VCH, Weinheim, **2018**.

[9] M. Parasram, V. Gevorgyan, *Chem. Soc. Rev.* **2017**, *46*, 6227–6240.

[10] A. Hossain, A. Bhattacharyya, O. Reiser, *Science* **2019**, *364*, eaav9713.

[11] V. Sathish, A. Ramdass, M. Velayudham, K.-L. Lu, P. Thanasekaran, S. Rajagopal, *Dalton Trans.* **2017**, *46*, 16738–16769.

[12] C. Rogers, M. O. Wolf, *Coord. Chem. Rev.* **2002**, *233–234*, 341–350.

[13] D.-L. Ma, H.-Z. He, K.-H. Leung, D. S.-H. Chan, C.-H. Leung, *Angew. Chem. Int. Ed.* **2013**, *52*, 7666–7682; *Angew. Chem.* **2013**, *125*, 7820–7837.

[14] C. E. Housecroft, E. C. Constable, *Chem. Sci.* **2022**, *13*, 1225–1262.

[15] I. Benesperi, R. Singh, M. Freitag, *Energies* **2020**, *13*, 2198.

[16] H. Huang, S. Banerjee, P. J. Sadler, *ChemBioChem* **2018**, *19*, 1574–1589.

[17] J. A. Gareth Williams, S. Develay, D. L. Rochester, L. Murphy, *Coord. Chem. Rev.* **2008**, *252*, 2596–2611.

[18] J. Shum, P. K.-K. Leung, K. K.-W. Lo, *Inorg. Chem.* **2019**, *58*, 2231–2247.

[19] V. W.-W. Yam, A. K.-W. Chan, E. Y.-H. Hong, *Nat. Chem. Rev.* **2020**, *4*, 528–541.

[20] Y. Chi, P.-T. Chou, *Chem. Soc. Rev.* **2010**, *39*, 638–655.

[21] R. D. Costa, E. Ortí, H. J. Bolink, F. Monti, G. Accorsi, N. Armaroli, *Angew. Chem. Int. Ed.* **2012**, *51*, 8178–8211; *Angew. Chem.* **2012**, *124*, 8300–8334.

[22] X. Li, Y. Xie, Z. Li, *Chem. Asian J.* **2021**, *16*, 2817–2829.

[23] V. W.-W. Yam, K. M.-C. Wong, *Chem. Commun.* **2011**, *47*, 11579–11592.

[24] F. H. Burstall, *J. Chem. Soc.* **1936**, 173–175.

[25] K. A. King, P. J. Spellane, R. J. Watts, *J. Am. Chem. Soc.* **1985**, *107*, 1431–1432.

[26] K. Suzuki, A. Kobayashi, S. Kaneko, K. Takehira, T. Yoshihara, H. Ishida, Y. Shiina, S. Oishi, S. Tobita, *Phys. Chem. Chem. Phys.* **2009**, *11*, 9850–9860.

[27] Z. Liu, Z. Bian, C. Huang in *Topics in Organometallic Chemistry, Vol. 28* (Eds.: H. Bozec, V. Guerchais), Springer, Berlin, **2010**, pp. 113–142.

[28] D. M. Roundhill in *Photochemistry and Photophysics of Metal Complexes* (Ed.: D. M. Roundhill), Springer, Boston, **1994**, pp. 165–215.

[29] D. M. Arias-Rotondo, J. K. McCusker in *Visible Light Photocatalysis in Organic Chemistry* (Eds.: C. Stephenson, T. Yoon, D. W. C. MacMillan), Wiley-VCH, Weinheim, **2018**, pp. 1–24.

[30] D. M. Arias-Rotondo, *Nat. Chem.* **2022**, *14*, 716.

[31] A. Juris, V. Balzani, F. Barigelletti, S. Campagna, P. Belser, A. von Zelewsky, *Coord. Chem. Rev.* **1988**, *84*, 85–277.

[32] O. S. Wenger, *Chem. Eur. J.* **2019**, *25*, 6043–6052.

[33] E. Bolton, M. M. Richter, *J. Chem. Educ.* **2001**, *78*, 47–48.

[34] D. W. Thompson, A. Ito, T. J. Meyer, *Pure Appl. Chem.* **2013**, *85*, 1257–1305.

[35] S. Zhang, Y. Ding, H. Wei, *Molecules* **2014**, *19*, 11933–11987.

[36] V. Balzani, P. Ceroni, A. Credi, M. Venturi, *Coord. Chem. Rev.* **2021**, *433*, 213758.

[37] C. Adachi, M. A. Baldo, S. R. Forrest, M. E. Thompson, *Appl. Phys. Lett.* **2000**, *77*, 904–906.

[38] T. Hofbeck, H. Yersin, *Inorg. Chem.* **2010**, *49*, 9290–9299.

[39] Y. You, S. Y. Park, *Dalton Trans.* **2009**, 1267–1282.

[40] M. K. Nazeeruddin, R. Humphry-Baker, D. Berner, S. Rivier, L. Zuppiroli, M. Graetzel, *J. Am. Chem. Soc.* **2003**, *125*, 8790–8797.

[41] K. Kalyanasundaram, *Coord. Chem. Rev.* **1982**, *46*, 159–244.

[42] P. S. Wagenknecht, P. C. Ford, *Coord. Chem. Rev.* **2011**, *255*, 591–616.

[43] *Topics in Current Chemistry, Vol. 281* (Eds.: V. Balzani, S. Campagna), Springer, Berlin, **2007**.

[44] C. Förster, K. Heinze, *Chem. Phys. Rev.* **2022**, *3*, 041302.

[45] P. Pyykkö, *Chem. Rev.* **1988**, *88*, 563–594.

[46] M. Kaupp, *J. Comput. Chem.* **2007**, *28*, 320–325.

[47] W. Gawelda, A. Cannizzo, V.-T. Pham, F. van Mourik, C. Bressler, M. Chergui, *J. Am. Chem. Soc.* **2007**, *129*, 8199–8206.

[48] M. Dorn, N. R. East, C. Förster, W. R. Kitzmann, J. Moll, F. Reichenauer, T. Reuter, L. Stein, K. Heinze in *Comprehensive Inorganic Chemistry III* (Ed.: J. Reedijk), Elsevier, San Diego, **2023**.

[49] W. R. Kitzmann, J. Moll, K. Heinze, *Photochem. Photobiol. Sci.* **2022**, *21*, 1309–1331.

[50] T. H. Maiman, *Nature* **1960**, *187*, 493–494.

[51] C. Degli Esposti, L. Bizzocchi, *J. Chem. Educ.* **2007**, *84*, 1316.

[52] R. S. Quimby, W. M. Yen, *J. Appl. Phys.* **1980**, *51*, 1780–1782.

[53] P. A. Scattergood in *Organometallic Chemistry, Vol. 43* (Eds.: N. J. Patmore, P. I. P. Elliott), Royal Society of Chemistry, Cambridge, **2020**, pp. 1–34.

[54] N. Serpone, M. A. Jamieson, M. S. Henry, M. Z. Hoffman, F. Bolletta, M. Maestri, *J. Am. Chem. Soc.* **1979**, *101*, 2907–2916.

[55] K. D. Barker, K. A. Barnett, S. M. Connell, J. W. Glaeser, A. J. Wallace, J. Wildsmith, B. J. Herbert, J. F. Wheeler, N. A. P. Kane-Maguire, *Inorg. Chim. Acta* **2001**, *316*, 41–49.

[56] L. S. Forster, *Chem. Rev.* **1990**, *90*, 331–353.

[57] L. S. Forster, *Coord. Chem. Rev.* **2002**, *227*, 59–92.

[58] A. D. Kirk, *Chem. Rev.* **1999**, *99*, 1607–1640.

[59] S. Otto, M. Grabolle, C. Förster, C. Kreitner, U. Resch-Genger, K. Heinze, *Angew. Chem. Int. Ed.* **2015**, *54*, 11572–11576; *Angew. Chem.* **2015**, *127*, 11735–11739.

[60] C. Wang, W. R. Kitzmann, F. Weigert, C. Förster, X. Wang, K. Heinze, U. Resch-Genger, *ChemPhotoChem* **2022**, *6*, e202100296.

[61] W. R. Kitzmann, C. Ramanan, R. Naumann, K. Heinze, *Dalton Trans.* **2022**, *51*, 6519–6525.

[62] S. Otto, M. Dorn, C. Förster, M. Bauer, M. Seitz, K. Heinze, *Coord. Chem. Rev.* **2018**, *359*, 102–111.

[63] F. Reichenauer, C. Wang, C. Förster, P. Boden, N. Ugur, R. Báez-Cruz, J. Kalmbach, L. M. Carrella, E. Rentschler, C. Ramanan, G. Niedner-Schatteburg, M. Gerhards, M. Seitz, U. Resch-Genger, K. Heinze, *J. Am. Chem. Soc.* **2021**, *143*, 11843–11855.

[64] J.-R. Jiménez, B. Doistau, C. M. Cruz, C. Besnard, J. M. Cuerva, A. G. Campaña, C. Piguet, *J. Am. Chem. Soc.* **2019**, *141*, 13244–13252.

[65] J.-R. Jiménez, M. Poncet, S. Míguez-Lago, S. Grass, J. Lacour, C. Besnard, J. M. Cuerva, A. G. Campaña, C. Piguet, *Angew.*

Chem. Int. Ed. **2021**, *60*, 10095–10102; *Angew. Chem.* **2021**, *133*, 10183–10190.

[66] S. Treiling, C. Wang, C. Förster, F. Reichenauer, J. Kalmbach, P. Boden, J. P. Harris, L. M. Carrella, E. Rentschler, U. Resch-Genger, C. Reber, M. Seitz, M. Gerhards, K. Heinze, *Angew. Chem. Int. Ed.* **2019**, *58*, 18075–18085; *Angew. Chem.* **2019**, *131*, 18243–18253.

[67] S. Otto, C. Förster, C. Wang, U. Resch-Genger, K. Heinze, *Chem. Eur. J.* **2018**, *24*, 12555–12563.

[68] J.-R. Jiménez, M. Poncet, B. Doistau, C. Besnard, C. Piguet, *Dalton Trans.* **2020**, *49*, 13528–13532.

[69] S. Sittel, R. Naumann, K. Heinze, *Front. Chem.* **2022**, *10*, 887439.

[70] M. Dorn, J. Kalmbach, P. Boden, A. Kruse, C. Dab, C. Reber, G. Niedner-Schatteburg, S. Lochbrunner, M. Gerhards, M. Seitz, K. Heinze, *Chem. Sci.* **2021**, *12*, 10780–10790.

[71] J. P. Zobel, T. Knoll, L. González, *Chem. Sci.* **2021**, *12*, 10791–10801.

[72] M. Dorn, J. Kalmbach, P. Boden, A. Päpcke, S. Gómez, C. Förster, F. Kuczelinis, L. M. Carrella, L. A. Büldt, N. H. Bings, E. Rentschler, S. Lochbrunner, L. González, M. Gerhards, M. Seitz, K. Heinze, *J. Am. Chem. Soc.* **2020**, *142*, 7947–7955.

[73] M. S. Fataftah, S. L. Bayliss, D. W. Laorenza, X. Wang, B. T. Phelan, C. B. Wilson, P. J. Mintun, B. D. Kovos, M. R. Wasielewski, S. Han, M. S. Sherwin, D. D. Awschalom, D. E. Freedman, *J. Am. Chem. Soc.* **2020**, *142*, 20400–20408.

[74] A. K. Mohammed, R. A. Isovitsch, A. W. Maverick, *Inorg. Chem.* **1998**, *37*, 2779–2785.

[75] Q. Yao, A. W. Maverick, *Inorg. Chem.* **1988**, *27*, 1669–1670.

[76] D. W. Laorenza, A. Kairalapova, S. L. Bayliss, T. Goldzak, S. M. Greene, L. R. Weiss, P. Deb, P. J. Mintun, K. A. Collins, D. D. Awschalom, T. C. Berkelbach, D. E. Freedman, *J. Am. Chem. Soc.* **2021**, *143*, 21350–21363.

[77] M. S. Fataftah, J. M. Zadrozny, S. C. Coste, M. J. Graham, D. M. Rogers, D. E. Freedman, *J. Am. Chem. Soc.* **2016**, *138*, 1344–1348.

[78] J. P. Harris, C. Reber, H. E. Colmer, T. A. Jackson, A. P. Forshaw, J. M. Smith, R. A. Kinney, J. Telser, *Can. J. Chem.* **2017**, *95*, 547–552.

[79] S. L. Bayliss, D. W. Laorenza, P. J. Mintun, B. D. Kovos, D. E. Freedman, D. D. Awschalom, *Science* **2020**, *370*, 1309–1312.

[80] *Photochemistry and Photophysics of Metal Complexes* (Ed.: D. M. Roundhill), Springer, Boston, **1994**.

[81] A. B. P. Lever, *Inorganic electronic spectroscopy*, 2. Ed., Elsevier, Amsterdam, **1984**.

[82] Z. Abedin-Siddique, T. Ohno, K. Nozaki, T. Tsubomura, *Inorg. Chem.* **2004**, *43*, 663–673.

[83] Y. Y. Chia, M. G. Tay, *Dalton Trans.* **2014**, *43*, 13159–13168.

[84] W.-P. To, G. Cheng, G. S. M. Tong, D. Zhou, C.-M. Che, *Front. Chem.* **2020**, *8*, 653.

[85] T. J. Penfold, E. Gindensperger, C. Daniel, C. M. Marian, *Chem. Rev.* **2018**, *118*, 6975–7025.

[86] G. Baryshnikov, B. Minaev, H. Ågren, *Chem. Rev.* **2017**, *117*, 6500–6537.

[87] J. van Houten, R. J. Watts, *J. Am. Chem. Soc.* **1976**, *98*, 4853–4858.

[88] A. Cannizzo, F. van Mourik, W. Gawelda, G. Zgrablic, C. Bressler, M. Chergui, *Angew. Chem. Int. Ed.* **2006**, *45*, 3174–3176; *Angew. Chem.* **2006**, *118*, 3246–3248.

[89] A. Soupart, F. Alary, J.-L. Heully, P. I. P. Elliott, I. M. Dixon, *Inorg. Chem.* **2020**, *59*, 14679–14695.

[90] S. Otto, J. P. Harris, K. Heinze, C. Reber, *Angew. Chem. Int. Ed.* **2018**, *57*, 11069–11073; *Angew. Chem.* **2018**, *130*, 11236–11240.

[91] J. N. Demas, D. G. Taylor, *Inorg. Chem.* **1979**, *18*, 3177–3179.

[92] N. H. Damrauer, G. Cerullo, A. Yeh, T. R. Boussie, C. V. Shank, J. K. McCusker, *Science* **1997**, *275*, 54–57.

[93] A. T. Yeh, C. V. Shank, J. K. McCusker, *Science* **2000**, *289*, 935–938.

[94] Z. Fang, A. Ito, S. Keinan, Z. Chen, Z. Watson, J. Rochette, Y. Kanai, D. Taylor, K. S. Schanze, T. J. Meyer, *Inorg. Chem.* **2013**, *52*, 8511–8520.

[95] Q. Sun, S. Mosquera-Vazquez, Y. Suffren, J. Hankache, N. Amstutz, L. M. Lawson Daku, E. Vauthey, A. Hauser, *Coord. Chem. Rev.* **2015**, *282–283*, 87–99.

[96] C. Kreitner, K. Heinze, *Dalton Trans.* **2016**, *45*, 13631–13647.

[97] F. Neese, *WIREs Comput. Mol. Sci.* **2012**, *2*, 73–78.

[98] F. Neese, *WIREs Comput. Mol. Sci.* **2022**, e1606.

[99] G. Auböck, M. Chergui, *Nat. Chem.* **2015**, *7*, 629–633.

[100] A. Cannizzo, C. J. Milne, C. Consani, W. Gawelda, C. Bressler, F. van Mourik, M. Chergui, *Coord. Chem. Rev.* **2010**, *254*, 2677–2686.

[101] L. A. Büldt, X. Guo, R. Vogel, A. Prescimone, O. S. Wenger, *J. Am. Chem. Soc.* **2017**, *139*, 985–992.

[102] C. Wegeberg, D. Häussinger, O. S. Wenger, *J. Am. Chem. Soc.* **2021**, *143*, 15800–15811.

[103] C. Wegeberg, O. S. Wenger, *Dalton Trans.* **2022**, *51*, 1297–1302.

[104] P. Herr, C. Kerzig, C. B. Larsen, D. Häussinger, O. S. Wenger, *Nat. Chem.* **2021**, *13*, 956–962.

[105] K. Heinze, *Nat. Chem.* **2021**, *13*, 926–928.

[106] W. Leis, M. A. Argüello Cordero, S. Lochbrunner, H. Schubert, A. Berkefeld, *J. Am. Chem. Soc.* **2022**, *144*, 1169–1173.

[107] Y. Zhang, J. L. Petersen, C. Milsmann, *J. Am. Chem. Soc.* **2016**, *138*, 13115–13118.

[108] Y. Zhang, T. S. Lee, J. L. Petersen, C. Milsmann, *J. Am. Chem. Soc.* **2018**, *140*, 5934–5947.

[109] Y. Zhang, T. S. Lee, J. M. Favale, D. C. Leary, J. L. Petersen, G. D. Scholes, F. N. Castellano, C. Milsmann, *Nat. Chem.* **2020**, *12*, 345–352.

[110] H. C. London, T. J. Whittemore, A. G. Gale, C. D. McMillen, D. Y. Pritchett, A. R. Myers, H. D. Thomas, G. C. Shields, P. S. Wagenknecht, *Inorg. Chem.* **2021**, *60*, 14399–14409.

[111] H. C. London, D. Y. Pritchett, J. A. Pienkos, C. D. McMillen, T. J. Whittemore, C. J. Bready, A. R. Myers, N. C. Vieira, S. Harold, G. C. Shields, P. S. Wagenknecht, *Inorg. Chem.* **2022**, *61*, 10986–10998.

[112] M. Iwamura, S. Takeuchi, T. Tahara, *Acc. Chem. Res.* **2015**, *48*, 782–791.

[113] R. Czerwieniec, M. J. Leitl, H. H. H. Homeier, H. Yersin, *Coord. Chem. Rev.* **2016**, *325*, 2–28.

[114] R. Czerwieniec, J. Yu, H. Yersin, *Inorg. Chem.* **2011**, *50*, 8293–8301.

[115] A. Barbieri, G. Accorsi, N. Armaroli, *Chem. Commun.* **2008**, 2185–2193.

[116] R. Hamze, J. L. Peltier, D. Sylvinson, M. Jung, J. Cardenas, R. Haiges, M. Soleilhavoup, R. Jazzar, P. I. Djurovich, G. Bertrand, M. E. Thompson, *Science* **2019**, *363*, 601–606.

[117] R. M. O'Donnell, T. A. Grusenmeyer, D. J. Stewart, T. R. Ensley, W. M. Shensky III, J. E. Haley, J. Shi, *Inorg. Chem.* **2017**, *56*, 9273–9280.

[118] B. Doistau, G. Collet, E. A. Bolomey, V. Sadat-Noorbakhsh, C. Besnard, C. Piguet, *Inorg. Chem.* **2018**, *57*, 14362–14373.

[119] O. Laporte, W. F. Meggers, *J. Opt. Soc. Am.* **1925**, *11*, 459.

[120] M. Brustolon, E. Giamello, *Electron Paramagnetic Resonance: A Practitioner's Toolkit*, John Wiley & Sons, Hoboken, **2009**.

[121] E. Previtera, A. Tissot, A. Hauser, *Eur. J. Inorg. Chem.* **2016**, 1972–1979.

[122] A. D. Kirk, C. Namasivayam, *J. Phys. Chem.* **1989**, *93*, 5488–5492.

[123] D. Ashen-Garry, M. Selke, *Photochem. Photobiol.* **2014**, *90*, 257–274.

[124] A. P. Darmanyan, J. W. Arbogast, C. S. Foote, *J. Phys. Chem.* **1991**, *95*, 7308–7312.

[125] M. Bregnhøj, M. Westberg, F. Jensen, P. R. Ogilby, *Phys. Chem. Chem. Phys.* **2016**, *18*, 22946–22961.

[126] T. S. Carlton, *J. Chem. Educ.* **2006**, *83*, 477–479.

[127] T. M. Stonelake, K. A. Phillips, H. Y. Otaif, Z. C. Edwardson, P. N. Horton, S. J. Coles, J. M. Beames, S. J. A. Pope, *Inorg. Chem.* **2020**, *59*, 2266–2277.

[128] J. A. Treadway, G. F. Strouse, R. R. Ruminski, T. J. Meyer, *Inorg. Chem.* **2001**, *40*, 4508–4509.

[129] D. B. Nemez, I. B. Lozada, J. D. Braun, J. A. Gareth Williams, D. E. Herbert, *Inorg. Chem.* **2022**, *61*, 13386–13398.

[130] H. Xiang, J. Cheng, X. Ma, X. Zhou, J. J. Chruma, *Chem. Soc. Rev.* **2013**, *42*, 6128–6185.

[131] M. J. Cook, A. P. Lewis, G. S. G. McAuliffe, V. Skarda, A. J. Thomson, J. L. Glasper, D. J. Robbins, *J. Chem. Soc. Perkin Trans. 2* **1984**, 1293–1301.

[132] J.-X. Liu, S.-L. Mei, X.-H. Chen, C.-J. Yao, *Crystals* **2021**, *11*, 155.

[133] S.-H. Wu, S. E. Burkhardt, J. Yao, Y.-W. Zhong, H. D. Abruña, *Inorg. Chem.* **2011**, *50*, 3959–3969.

[134] S. D. Bergman, D. Gut, M. Kol, C. Sabatini, A. Barbieri, F. Barigelletti, *Inorg. Chem.* **2005**, *44*, 7943–7950.

[135] R. Englman, J. Jortner, *Mol. Phys.* **1970**, *18*, 145–164.

[136] C.-H. Yang, M. Mauro, F. Polo, S. Watanabe, I. Muenster, R. Fröhlich, L. de Cola, *Chem. Mater.* **2012**, *24*, 3684–3695.

[137] S. DiLuzio, V. Mdluli, T. U. Connell, J. Lewis, V. VanBenschoten, S. Bernhard, *J. Am. Chem. Soc.* **2021**, *143*, 1179–1194.

[138] M. S. Mehata, Y. Yang, Z.-J. Qu, J.-S. Chen, F.-J. Zhao, K.-L. Han, *RSC Adv.* **2015**, *5*, 34094–34099.

[139] L. Stein, P. Boden, R. Naumann, C. Förster, G. Niedner-Schatteburg, K. Heinze, *Chem. Commun.* **2022**, *58*, 3701–3704.

[140] S. Sun, W. Sun, D. Mu, N. Jiang, X. Peng, *Chem. Commun.* **2015**, *51*, 2529–2531.

[141] C. K. Jørgensen in *Advances in Chemical Physics, Vol. 5* (Ed.: I. Prigogine), John Wiley & Sons, New York, **1963**, pp. 33–146.

[142] N. Sinha, J.-R. Jiménez, B. Pfund, A. Prescimone, C. Piguet, O. S. Wenger, *Angew. Chem. Int. Ed.* **2021**, *60*, 23722–23728; *Angew. Chem.* **2021**, *133*, 23915–23921.

[143] N. Sawicka, C. J. Craze, P. N. Horton, S. J. Coles, E. Richards, S. J. A. Pope, *Chem. Commun.* **2022**, *58*, 5733–5736.

[144] H. L. Schläfer, H. Gausmann, H. Witzke, *J. Mol. Spectrosc.* **1966**, *21*, 125–129.

[145] R. D. Dill, R. I. Portillo, S. G. Shepard, M. P. Shores, A. K. Rappé, N. H. Damrauer, *Inorg. Chem.* **2020**, *59*, 14706–14715.

[146] A. C. Sell, J. C. Wetzel, M. Schmitz, A. W. Maijenburg, G. Woltersdorf, R. Naumann, C. Kerzig, *Dalton Trans.* **2022**, *51*, 10799–10808.

[147] J.-H. Lee, C.-H. Chen, P.-H. Lee, H.-Y. Lin, M. Leung, T.-L. Chiu, C.-F. Lin, *J. Mater. Chem. C* **2019**, *7*, 5874–5888.

[148] J. A. Treadway, B. Loeb, R. Lopez, P. A. Anderson, F. R. Keene, T. J. Meyer, *Inorg. Chem.* **1996**, *35*, 2242–2246.

[149] M. Wada, S. Ito, H. Uno, T. Murashima, N. Ono, T. Urano, Y. Urano, *Tetrahedron Lett.* **2001**, *42*, 6711–6713.

[150] P. Herr, F. Glaser, L. A. Büldt, C. B. Larsen, O. S. Wenger, *J. Am. Chem. Soc.* **2019**, *141*, 14394–14402.

[151] M. W. Perkovic, M. J. Heeg, J. F. Endicott, *Inorg. Chem.* **1991**, *30*, 3140–3147.

[152] A. M. McDaniel, H.-W. Tseng, E. A. Hill, N. H. Damrauer, A. K. Rappé, M. P. Shores, *Inorg. Chem.* **2013**, *52*, 1368–1378.

[153] A. Breivogel, C. Förster, K. Heinze, *Inorg. Chem.* **2010**, *49*, 7052–7056.

[154] M. F. K. Trautnitz, C. Doffek, M. Seitz, *ChemPhysChem* **2019**, *20*, 2179–2186.

[155] W. Browne, J. G. Vos, *Coord. Chem. Rev.* **2001**, *219–221*, 761–787.

[156] C. Wang, S. Otto, M. Dorn, E. Kreidt, J. Lebon, L. Sršan, P. Di Martino-Fumo, M. Gerhards, U. Resch-Genger, M. Seitz, K. Heinze, *Angew. Chem. Int. Ed.* **2018**, *57*, 1112–1116; *Angew. Chem.* **2018**, *130*, 1125–1130.

[157] S. F. McClanahan, J. R. Kincaid, *J. Am. Chem. Soc.* **1986**, *108*, 3840–3841.

[158] G. J. Wilson, W. H. F. Sasse, A. W.-H. Mau, *Chem. Phys. Lett.* **1996**, *250*, 583–588.

[159] D. S. Tyson, J. Bialecki, F. N. Castellano, *Chem. Commun.* **2000**, 2355–2356.

[160] M. Hissler, A. Harriman, A. Khatyr, R. Ziessel, *Chem. Eur. J.* **1999**, *5*, 3366–3381.

[161] N. D. McClenaghan, Y. Leydet, B. Maubert, M. T. Indelli, S. Campagna, *Coord. Chem. Rev.* **2005**, *249*, 1336–1350.

[162] A. J. Howarth, M. B. Majewski, M. O. Wolf, *Coord. Chem. Rev.* **2015**, *282–283*, 139–149.

[163] J. Langelaar, R. P. H. Rettschnick, G. J. Hoijtink, *J. Chem. Phys.* **1971**, *54*, 1–7.

[164] C. Wang, F. Reichenauer, W. R. Kitzmann, C. Kerzig, K. Heinze, U. Resch-Genger, *Angew. Chem. Int. Ed.* **2022**, *61*, e202202238; *Angew. Chem.* **2022**, *134*, e202202238.

[165] P. A. Scattergood, A. M. Ranieri, L. Charalambou, A. Comia, D. A. W. Ross, C. R. Rice, S. J. O. Hardman, J.-L. Heully, I. M. Dixon, M. Massi, F. Alary, P. I. P. Elliott, *Inorg. Chem.* **2020**, *59*, 1785–1803.

[166] F. Geist, A. Jackel, R. F. Winter, *Inorg. Chem.* **2015**, *54*, 10946–10957.

[167] A. S. Gowda, T. S. Lee, M. C. Rosko, J. L. Petersen, F. N. Castellano, C. Milsmann, *Inorg. Chem.* **2022**, *61*, 7338–7348.

[168] E. V. Puttock, A. Sil, D. S. Yufit, J. A. Gareth Williams, *Dalton Trans.* **2020**, *49*, 10463–10476.

[169] P. Pander, R. Daniels, A. V. Zaytsev, A. Horn, A. Sil, T. J. Penfold, J. A. Gareth Williams, V. N. Kozhevnikov, F. B. Dias, *Chem. Sci.* **2021**, *12*, 6172–6180.

[170] C. E. Housecroft, E. C. Constable, *J. Mater. Chem. C* **2022**, *10*, 4456–4482.

[171] T. Hofbeck, U. Monkowius, H. Yersin, *J. Am. Chem. Soc.* **2015**, *137*, 399–404.

[172] P. Li, Z. Wang, S. Wang, C. Zhou, Y. Zhang, C. Zheng, R. Chen, *J. Phys. Chem. C* **2021**, *125*, 26770–26777.

[173] K. Li, Y. Chen, J. Wang, C. Yang, *Coord. Chem. Rev.* **2021**, *433*, 213755.

[174] G. Li, Z.-Q. Zhu, Q. Chen, J. Li, *Org. Electron.* **2019**, *69*, 135–152.

[175] R. Gómez-Bombarelli, J. Aguilera-Iparraguirre, T. D. Hirzel, D. Duvenaud, D. Maclaurin, M. A. Blood-Forsythe, H. S. Chae, M. Einzinger, D.-G. Ha, T. Wu, G. Markopoulos, S. Jeon, H. Kang, H. Miyazaki, M. Numata, S. Kim, W. Huang, S. I. Hong, M. Baldo, R. P. Adams, A. Aspuru-Guzik, *Nat. Mater.* **2016**, *15*, 1120–1127.

[176] H. U. Güdel, T. R. Snellgrove, *Inorg. Chem.* **1978**, *17*, 1617–1620.

[177] A. W. Adamson, *J. Phys. Chem.* **1967**, *71*, 798–808.

[178] S. Otto, N. Scholz, T. Behnke, U. Resch-Genger, K. Heinze, *Chem. Eur. J.* **2017**, *23*, 12131–12135.

[179] C. Wang, S. Otto, M. Dorn, K. Heinze, U. Resch-Genger, *Anal. Chem.* **2019**, *91*, 2337–2344.

[180] G. D. Hager, R. J. Watts, G. A. Crosby, *J. Am. Chem. Soc.* **1975**, *97*, 7037–7042.

[181] M. L. Fetterolf, H. W. Offen, *J. Phys. Chem.* **1985**, *89*, 3320–3323.

[182] Y. R. Shen, K. L. Bray, *Phys. Rev. B* **1997**, *56*, 10882–10891.

[183] J. W. Kenney III, J. W. Clymire, S. F. Agnew, *J. Am. Chem. Soc.* **1995**, *117*, 1645–1646.

[184] H. Yersin, E. Gallhuber, *Inorg. Chem.* **1984**, *23*, 3745–3748.

[185] E. Krausz, J. Ferguson in *Progress in Inorganic Chemistry, Vol. 37* (Ed.: S. J. Lippard), John Wiley & Sons, Hoboken, **1989**, pp. 293–390.

[186] H. G. Drickamer, J. M. Lang, Z. A. Dreger, *Russ. Chem. Bull.* **1995**, *44*, 1149–1155.

[187] J. M. Lang, Z. A. Dreger, H. G. Drickamer, *J. Phys. Chem.* **1993**, *97*, 2289–2294.

[188] G. J. Piermarini, S. Block, J. D. Barnett, R. A. Forman, *J. Appl. Phys.* **1975**, *46*, 2774–2780.

[189] R. A. Forman, G. J. Piermarini, J. D. Barnett, S. Block, *Science* **1972**, *176*, 284–285.

[190] H.-T. Macholdt, R. van Eldik, H. Kelm, H. Elias, *Inorg. Chim. Acta* **1985**, *104*, 115–118.

[191] A. Pannwitz, S. Poirier, N. Bélanger-Desmarais, A. Prescimone, O. S. Wenger, C. Reber, *Chem. Eur. J.* **2018**, *24*, 7830–7833.

[192] P. Chen, T. J. Meyer, *Chem. Rev.* **1998**, *98*, 1439–1478.

[193] E. M. Kober, B. P. Sullivan, T. J. Meyer, *Inorg. Chem.* **1984**, *23*, 2098–2104.

[194] S. D. Helland, A. S. Chang, K. W. Lee, P. S. Hutchison, W. W. Brennessel, W. T. Eckenhoff, *Inorg. Chem.* **2020**, *59*, 705–716.

[195] W. Kaim, S. Kohlmann, S. Ernst, B. Olbrich-Deussner, C. Bessenbacher, A. Schulz, *J. Organomet. Chem.* **1987**, *321*, 215–226.

[196] N. M. Ali, V. L. MacLeod, P. Jennison, I. V. Sazanovich, C. A. Hunter, J. A. Weinstein, M. D. Ward, *Dalton Trans.* **2012**, *41*, 2408–2419.

[197] D. M. Manuta, A. J. Lees, *Inorg. Chem.* **1983**, *22*, 3825–3828.

[198] S. Nigam, S. Rutan, *Appl. Spectrosc.* **2001**, *55*, 362A–370A.

[199] C. Reichardt, *Chem. Rev.* **1994**, *94*, 2319–2358.

[200] L. Fodor, G. Lendvay, A. Horváth, *J. Phys. Chem. A* **2007**, *111*, 12891–12900.

[201] J. D. Earley, A. Zieleniewska, H. H. Ripberger, N. Y. Shin, M. S. Lazorski, Z. J. Mast, H. J. Sayre, J. K. McCusker, G. D. Scholes, R. R. Knowles, O. G. Reid, G. Rumbles, *Nat. Chem.* **2022**, *14*, 746–753.

[202] E. P. Farney, S. J. Chapman, W. B. Swords, M. D. Torelli, R. J. Hamers, T. P. Yoon, *J. Am. Chem. Soc.* **2019**, *141*, 6385–6391.

[203] R. Mondal, I. B. Lozada, R. L. Davis, J. A. Gareth Williams, D. E. Herbert, *J. Mater. Chem. C* **2019**, *7*, 3772–3778.

[204] Y. Ma, Y. Dong, P. She, S. Liu, M. Xie, Y. Yu, Y. Li, Q. Zhao, W. Huang, *Adv. Opt. Mater.* **2018**, *6*, 1801065.

[205] Y. Zhu, Y. Ma, J. Zhu, *J. Lumin.* **2013**, *137*, 198–203.

[206] D. Ma, L. Duan, Y. Wei, L. He, L. Wang, Y. Qiu, *Chem. Commun.* **2014**, *50*, 530–532.

[207] M. S. Henry, *J. Am. Chem. Soc.* **1977**, *99*, 6138–6139.

[208] M. C. DeRosa, R. J. Crutchley, *Coord. Chem. Rev.* **2002**, *233–234*, 351–371.

[209] M.-A. Schmid, J. Brückmann, J. Bösking, D. Nauroozi, M. Karnahl, S. Rau, S. Tschierlei, *Chem. Eur. J.* **2022**, *28*, e202103609.

[210] S. Otto, A. M. Nauth, E. Ermilov, N. Scholz, A. Friedrich, U. Resch-Genger, S. Lochbrunner, T. Opatz, K. Heinze, *ChemPhotoChem* **2017**, *1*, 344–349.

[211] C. Grundke, R. C. Silva, W. R. Kitzmann, K. Heinze, K. T. de Oliveira, T. Opatz, *J. Org. Chem.* **2022**, *87*, 5630–5642.

[212] U. Basu, S. Otto, K. Heinze, G. Gasser, *Eur. J. Inorg. Chem.* **2019**, 37–41.

[213] S. Monro, K. L. Colón, H. Yin, J. Roque, P. Konda, S. Gujar, R. P. Thummel, L. Lilge, C. G. Cameron, S. A. McFarland, *Chem. Rev.* **2019**, *119*, 797–828.

[214] M. A. Filatov in *Detection Science, Vol. 11* (Eds.: D. B. Papkovsky, R. I. Dmitriev), Royal Society of Chemistry, Cambridge, **2018**, pp. 91–116.

[215] L. Stein, C. Wang, U. Resch-Genger, K. Heinze, *Dalton Trans.* **2022**, *51*, 17664–17670.

[216] M. Wrighton, D. L. Morse, *J. Am. Chem. Soc.* **1974**, *96*, 998–1003.

[217] A. Harriman, *J. Chem. Soc. Chem. Commun.* **1977**, 777–778.

[218] G. A. Crosby, W. G. Perkins, D. M. Klassen, *J. Chem. Phys.* **1965**, *43*, 1498–1503.

[219] E. L. Sciuto, M. F. Santangelo, G. Villaggio, F. Sinatra, C. Bongiorno, G. Nicotra, S. Libertino, *Sens. Bio.-Sens. Res.* **2015**, *6*, 67–71.

[220] W. E. Jones, M. A. Fox, *J. Phys. Chem.* **1994**, *98*, 5095–5099.

[221] J. L. Brennan, T. E. Keyes, R. J. Forster, *Langmuir* **2006**, *22*, 10754–10761.

[222] J. R. Lakowicz, *Principles of fluorescence spectroscopy*, 3. Ed., Springer, New York, **2010**.

[223] T. H. Bürgin, F. Glaser, O. S. Wenger, *J. Am. Chem. Soc.* **2022**, *144*, 14181–14194.

[224] L. A. Büldt, X. Guo, A. Prescimone, O. S. Wenger, *Angew. Chem. Int. Ed.* **2016**, *55*, 11247–11250; *Angew. Chem.* **2016**, *128*, 11413–11417.

[225] K.-T. Yeung, W.-P. To, C. Sun, G. Cheng, C. Ma, G. S. M. Tong, C. Yang, C.-M. Che, *Angew. Chem. Int. Ed.* **2017**, *56*, 133–137; *Angew. Chem.* **2017**, *129*, 139–143.

[226] D. Yu, W.-P. To, G. S. M. Tong, L.-L. Wu, K.-T. Chan, L. Du, D. L. Phillips, Y. Liu, C.-M. Che, *Chem. Sci.* **2020**, *11*, 6370–6382.

[227] S. M. Stevenson, M. P. Shores, E. M. Ferreira, *Angew. Chem. Int. Ed.* **2015**, *54*, 6506–6510; *Angew. Chem.* **2015**, *127*, 6606–6610.

[228] R. F. Higgins, S. M. Fatur, S. G. Shepard, S. M. Stevenson, D. J. Boston, E. M. Ferreira, N. H. Damrauer, A. K. Rappé, M. P. Shores, *J. Am. Chem. Soc.* **2016**, *138*, 5451–5464.

[229] R. F. Higgins, S. M. Fatur, N. H. Damrauer, E. M. Ferreira, A. K. Rappé, M. P. Shores, *ACS Catal.* **2018**, *8*, 9216–9225.

[230] S. M. Stevenson, R. F. Higgins, M. P. Shores, E. M. Ferreira, *Chem. Sci.* **2017**, *8*, 654–660.

[231] F. A. Baptista, D. Krizsan, M. Stitch, I. V. Sazanovich, I. P. Clark, M. Towrie, C. Long, L. Martinez-Fernandez, R. Improta, N. A. P. Kane-Maguire, J. M. Kelly, S. J. Quinn, *J. Am. Chem. Soc.* **2021**, *143*, 14766–14779.

[232] L. Schmid, C. Kerzig, A. Prescimone, O. S. Wenger, *JACS Au* **2021**, *1*, 819–832.

[233] P. M. Becker, C. Förster, L. M. Carrella, P. Boden, D. Hunger, J. van Slageren, M. Gerhards, E. Rentschler, K. Heinze, *Chem. Eur. J.* **2020**, *26*, 7199–7204.

[234] C. Förster, M. Dorn, T. Reuter, G. Davarci, T. Reich, L. Carrella, E. Rentschler, K. Heinze, *Inorganics* **2018**, *6*, 86.

[235] Y. Cheng, Y. Yang, Y. Qu, P. Li, *Org. Lett.* **2012**, *14*, 98–101.

[236] S. Ji, W. Wu, W. Wu, H. Guo, J. Zhao, *Angew. Chem. Int. Ed.* **2011**, *50*, 1626–1629; *Angew. Chem.* **2011**, *123*, 1664–1667.

[237] A. Gafni, I. Z. Steinberg, *Isr. J. Chem.* **1976**, *15*, 102–105.

[238] L. Arrico, L. Di Bari, F. Zinna, *Chem. Eur. J.* **2021**, *27*, 2920–2934.

[239] C. Dee, F. Zinna, W. R. Kitzmann, G. Pescitelli, K. Heinze, L. Di Bari, M. Seitz, *Chem. Commun.* **2019**, *55*, 13078–13081.

[240] R. T. Watson, N. Desai, J. Wildsmith, J. F. Wheeler, N. A. P. Kane-Maguire, *Inorg. Chem.* **1999**, *38*, 2683–2687.

[241] V. G. Vaidyanathan, B. U. Nair, *Eur. J. Inorg. Chem.* **2004**, 1840–1846.

[242] F. Strieth-Kalthoff, M. J. James, M. Teders, L. Pitzer, F. Glorius, *Chem. Soc. Rev.* **2018**, *47*, 7190–7202.

[243] F. Strieth-Kalthoff, F. Glorius, *Chem* **2020**, *6*, 1888–1903.

[244] T. N. Singh-Rachford, F. N. Castellano, *Coord. Chem. Rev.* **2010**, *254*, 2560–2573.

[245] J. Zhao, S. Ji, H. Guo, *RSC Adv.* **2011**, *1*, 937.

[246] R. R. Islangulov, F. N. Castellano, *Angew. Chem. Int. Ed.* **2006**, *45*, 5957–5959; *Angew. Chem.* **2006**, *118*, 6103–6105.

[247] B. Jing, T. Wu, C. Tian, M. Zhang, T. Shen, *Bull. Chem. Soc. Jpn.* **2000**, *73*, 1749–1755.

[248] C. Müller, D. Isakov, S. Rau, B. Dietzek, *J. Phys. Chem. A* **2021**, *125*, 5911–5921.

[249] T.-T. Meng, H. Wang, Z.-B. Zheng, K.-Z. Wang, *Inorg. Chem.* **2017**, *56*, 4775–4779.

[250] L. Tormo, N. Bustamante, G. Colmenarejo, G. Orellana, *Anal. Chem.* **2010**, *82*, 5195–5204.

[251] S. J. Payne, G. L. Fiore, C. L. Fraser, J. N. Demas, *Anal. Chem.* **2010**, *82*, 917–921.

[252] J. W. Kenney III, J. J. Lee, *Chemosensors* **2021**, *9*, 109.

[253] M. Wu, Z. Zhang, J. Yong, P. M. Schenk, D. Tian, Z. P. Xu, R. Zhang, *Top. Curr. Chem.* **2022**, *380*, 29.

[254] J. Ru, X. Mi, L. Guan, X. Tang, Z. Ju, G. Zhang, C. Wang, W. Liu, *J. Mater. Chem. B* **2015**, *3*, 6205–6212.

[255] D.-W. Zhang, M. Li, C.-F. Chen, *Chem. Soc. Rev.* **2020**, *49*, 1331–1343.

[256] J. P. Riehl, F. S. Richardson, *Chem. Rev.* **1986**, *86*, 1–14.

[257] N. F. M. Mukthar, N. D. Schley, G. Ung, *J. Am. Chem. Soc.* **2022**, *144*, 6148–6153.

[258] S. C. J. Meskers, *ChemPhotoChem* **2022**, *6*, e202100154.

[259] J. Kumar, T. Nakashima, T. Kawai, *J. Phys. Chem. Lett.* **2015**, *6*, 3445–3452.

[260] J. Gong, X. Zhang, *Coord. Chem. Rev.* **2022**, *453*, 214329.

[261] L. E. MacKenzie, R. Pal, *Nat. Rev. Chem.* **2021**, *5*, 109–124.

[262] P. Stachelek, L. MacKenzie, D. Parker, R. Pal, *Nat. Commun.* **2022**, *13*, 553.

[263] Y. Deng, M. Wang, Y. Zhuang, S. Liu, W. Huang, Q. Zhao, *Light: Sci. Appl.* **2021**, *10*, 76.

[264] E. Kreidt, L. Arrico, F. Zinna, L. Di Bari, M. Seitz, *Chem. Eur. J.* **2018**, *24*, 13556–13564.

[265] M. Poncet, A. Benchohra, J.-R. Jiménez, C. Piguet, *ChemPhotoChem* **2021**, *5*, 880–892.

[266] B. Doistau, J.-R. Jiménez, C. Piguet, *Front. Chem.* **2020**, *8*, 555.

[267] R. Aoki, R. Toyoda, J. F. Kögel, R. Sakamoto, J. Kumar, Y. Kitagawa, K. Harano, T. Kawai, H. Nishihara, *J. Am. Chem. Soc.* **2017**, *139*, 16024–16027.

[268] J. F. Kögel, S. Kusaka, R. Sakamoto, T. Iwashima, M. Tsuchiya, R. Toyoda, R. Matsuoka, T. Tsukamoto, J. Yuasa, Y. Kitagawa, T. Kawai, H. Nishihara, *Angew. Chem. Int. Ed.* **2016**, *55*, 1377–1381; *Angew. Chem.* **2016**, *128*, 1399–1403.

[269] N. Sinha, B. Pfund, C. Wegeberg, A. Prescimone, O. S. Wenger, *J. Am. Chem. Soc.* **2022**, *144*, 9859–9873.

[270] H. Yoon, Y.-M. Lee, X. Wu, K.-B. Cho, R. Sarangi, W. Nam, S. Fukuzumi, *J. Am. Chem. Soc.* **2013**, *135*, 9186–9194.

[271] P. Chábera, Y. Liu, O. Prakash, E. Thyrhaug, A. E. Nahhas, A. Honarfar, S. Essén, L. A. Fredin, T. C. B. Harlang, K. S. Kjær, K. Handrup, F. Ericson, H. Tatsuno, K. Morgan, J. Schnadt, L. Häggström, T. Ericsson, A. Sobkowiak, S. Lidin, P. Huang, S. Styring, J. Uhlig, J. Bendix, R. Lomoth, V. Sundström, P. Persson, K. Wärnmark, *Nature* **2017**, *543*, 695–699.

[272] K. S. Kjær, N. Kaul, O. Prakash, P. Chábera, N. W. Rose-mann, A. Honarfar, O. Gordivska, L. A. Fredin, K.-E. Bergquist, L. Häggström, T. Ericsson, L. Lindh, A. Yartsev, S. Styring, P. Huang, J. Uhlig, J. Bendix, D. Strand, V. Sundström, P. Persson, R. Lomoth, K. Wärnmark, *Science* **2019**, *363*, 249–253.

[273] M. Grübel, I. Bosque, P. J. Altmann, T. Bach, C. R. Hess, *Chem. Sci.* **2018**, *9*, 3313–3317.

[274] Y. Zhang, D. C. Leary, A. M. Belldina, J. L. Petersen, C. Milsmann, *Inorg. Chem.* **2020**, *59*, 14716–14730.

[275] S. Kaufhold, N. W. Rosemann, P. Chábera, L. Lindh, I. Bolaño Losada, J. Uhlig, T. Pascher, D. Strand, K. Wärnmark, A. Yartsev, P. Persson, *J. Am. Chem. Soc.* **2021**, *143*, 1307–1312.

[276] A. K. Pal, C. Li, G. S. Hanan, E. Zysman-Colman, *Angew. Chem. Int. Ed.* **2018**, *57*, 8027–8031; *Angew. Chem.* **2018**, *130*, 8159–8163.

[277] P. Herr, A. Schwab, S. Kupfer, O. S. Wenger, *ChemPhotoChem* **2022**, *6*, e202200052.

[278] J.-R. Jiménez, B. Doistau, C. Besnard, C. Piguet, *Chem. Commun.* **2018**, *54*, 13228–13231.

[279] J. Chong, C. Besnard, C. M. Cruz, C. Piguet, J.-R. Jiménez, *Dalton Trans.* **2022**, *51*, 4297–4309.

[280] J. Kalmbach, C. Wang, Y. You, C. Förster, H. Schubert, K. Heinze, U. Resch-Genger, M. Seitz, *Angew. Chem. Int. Ed.* **2020**, *59*, 18804–18808; *Angew. Chem.* **2020**, *132*, 18966–18970.

[281] P. Boden, P. Di Martino-Fumo, G. Niedner-Schatteburg, W. Seidel, K. Heinze, M. Gerhards, *Phys. Chem. Chem. Phys.* **2021**, *23*, 13808–13818.

Reviews

W. R. Kitzmann, K. Heinze* _ e202213207

Charge-Transfer and Spin-Flip States: Thriving as Complements
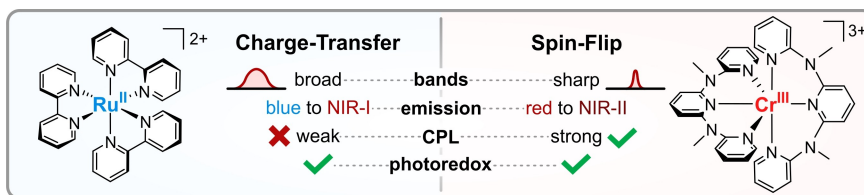
Charge-transfer excited states have been at the focus of inorganic photochemistry for decades, together with their strongest opponents: detrimental metal-centered states. In recent years, interest in metal-centered spin-flip states was reignited by a new type of photoactive chromium(III) complex. This Review delineates similarities and unique features of charge-transfer and spin-flip states, from fundamentals to applications.